VIDEO TRANSMISSION OVER LTE-UNLICENSED

by

Fatema Mahmood Aseeri

A Thesis Presented to the Faculty of the
American University of Sharjah
College of Engineering
in Partial Fulfillment
of the Requirements
for the Degree of

Master of Science in
Electrical Engineering

Sharjah, United Arab Emirates

November 2017

Approval Signatures

We, the undersigned, approve the Master's Thesis of Fatema Mahmood Aseeri

Thesis Title: Video Transmission over LTE-Unlicensed.

Signature	**Date of Signature** (dd/mm/yyyy)
___________________________ Dr. Mohamed Hassan Professor, Department of Electrical Engineering Thesis Advisor	_______________
___________________________ Dr. Mahmoud H. Ismail Associate Professor, Department of Electrical Engineering Thesis Co. Advisor	_______________
___________________________ Dr. Taha Landolsi Professor, Department of Computer Science and Engineering Thesis Committee Member	_______________
___________________________ Dr. Hasan Mir Associate Professor, Department of Electrical Engineering Thesis Committee Member	_______________
___________________________ Dr. Nasser Qaddoumi Department Head, Department of Electrical Engineering	_______________
___________________________ Dr. Ghaleb Husseini Associate Dean for Graduate Affairs and Research College of Engineering	_______________
___________________________ Dr. Richard Schoephoerster Dean, College of Engineering	_______________
___________________________ Dr. Mohamed El-Tarhuni Vice Provost for Graduate Studies	_______________

Acknowledgements

I would like to thank my advisors, Dr. Mohamed Hassan and Dr. Mahmoud H. Ismail, for their continuous support and valued guidance that has improved this work beyond my initial vision.

I would also like to thank the Department of Electrical Engineering at the American University of Sharjah for supporting this research and offering me the Graduate Teaching Assistanship that has allowed me to continue my higher education.

Finally, my thanks go to my family and friends for their continuous presence and unconditional support.

To my parents, for their unending love and support . . .

Abstract

The witnessed proliferation in the demand on wireless spectrum over the past years is anticipated to lead to a bandwidth scarcity problem. The situation is further aggravated by the combined increase in the demand on the delivery of high definition multimedia content over wireless networks. Recently, it was proposed to extend the LTE operation into the unlicensed spectrum (LTE-U) in an attempt to mitigate the expected scarcity problem. However, extending the operation of LTE to the unlicensed spectrum is expected to degrade the performance of other incumbent technologies, especially WiFi. While several LTE-U channel access mechanisms for enabling the coexistence of LTE with WiFi, in the unlicensed spectrum, have been proposed and evaluated, very few addressed the problem of video streaming over LTE-U. Therefore, this thesis further explores the design of efficient LTE-U channel access mechanisms from the perspective of video streaming. Specifically, we propose two channel selection schemes for video transmission over LTE-U. The first is a static channel selection scheme in which the LTE-U user equipment (UEs) are assigned to channels based on their frame type. The second one is an adaptive channel selection scheme in which UE frames are assigned to channels based on the solution to a multi-objective optimization problem that takes into account the UE's Quality of Experience (QoE) requirements while striving to minimize the interference caused to WiFi. Simulation results show that, compared to a scheme that employs an effective channel access mechanism but assigns frames to channels randomly, our proposed QoE-based channel selection scheme achieves a considerably better performance, in terms of improving the received video quality and reducing the inter-frame delay for both LTE-U and WiFi users. These results confirm the conclusion that while extending the operation of LTE-U to the unlicensed spectrum does indeed come with great benefits for LTE networks, that extension should be accompanied by smart channel selection schemes that take both the nature of the UEs data and the channel conditions into account.

Search Terms: ***Long-Term Evolution (LTE), LTE-Unlicensed (LTE-U), video transmission, channel selection.***

Table of Contents

Abstract 6

List of Figures 10

List of Tables 12

List of Abbreviations 13

Chapter 1: Introduction 16

1.1 Background 20

1.1.1 LTE 20

1.1.1.1 Network architecture 21

1.1.1.2 Physical layer 21

1.1.1.3 Scheduling 23

1.1.2 WiFi 24

1.1.3 Digital video compression 26

1.1.3.1 Intra-frame coding 27

1.1.3.2 Inter-frame coding 28

1.1.3.3 Video qulaity assessment 30

Chapter 2: Literature Review 33

2.1 LBT-Based Channel Access Mechanisms 33

2.1.1 Modifications to the current LBT back-off mechanism 34

2.1.2 Channel sensing schemes 35

2.1.3 LTE-U idle times 36

2.2 Non-LBT Channel Access Mechanisms 37

2.2.1 Time-division multiplexing techniques 38

2.2.2 Channel selection techniques 38

2.2.3 Power control techniques 39

2.2.4 Game-based coexistence schemes 39

2.2.5 Unified control of LTE-U and WiFi channel access 40

2.3 Traffic Balancing 41
2.4 Resource Allocation and Scheduling 42
2.5 Additional Aspects of LTE-U Operation 44
2.6 Surveys and Comparative Studies of Different Coexistence Mechanisms . 45
2.7 Video Transmission Over Cellular Networks 46
2.7.1 Resource allocation and scheduling algorithms 46
2.7.2 SVC video transmission 47
2.7.3 Cross layer designs 49
2.7.4 Analytical models for error control techniques and received video quality 49
2.7.5 Video delivery architectures 50
Chapter 3: Frame Type-Based Channel Access 52
3.1 Proposed Approach 52
3.1.1 Modified LBT channel access 54
3.1.2 Adaptive *p*-persistent CSMA channel access 55
3.2 Performance Evaluation 57
3.2.1 Simulation scenario 57
3.2.2 Simulation results 58
Chapter 4: QoE-Based Dynamic Channel Selection 64
4.1 Proposed Approach 64
4.1.1 SNR-based PSNR prediction framework 65
4.1.2 Frame delay prediction 72
4.1.3 Coexistence with WiFi 73
4.1.4 Channel selection optimization problem 74
4.2 Performance Evaluation 76
4.2.1 Simulation scenario 77
4.2.2 Simulation results 79
Chapter 5: Conclusion 84

References 86

Vita 92

List of Figures

Figure 1: Global mobile data traffic, 2016 to 2021 [1]. 16

Figure 2: Global mobile data traffic based on connection type [1]. 17

Figure 3: Mobile data traffic breakdown based on content type [1]. 20

Figure 4: LTE network structure. 22

Figure 5: OFDMA: The allocation of time-frequency resources to different UEs. 23

Figure 6: WiFi network structure. 25

Figure 7: Carrier sense multiple access with collision avoidance. 26

Figure 8: Block diagram for JPEG compression. 27

Figure 9: Block diagram for motion estimation and compensation. 29

Figure 10: A typical GOP structure. 30

Figure 11: Modified LBT channel access mechanism. 55

Figure 12: Flow chart for the adaptive p-persistent CSMA channel access. 56

Figure 13: System model for the frame type-based channel access. 57

Figure 14: Spectrum crunch resulting from increasing the number of LTE UEs in the licensed spectrum. 59

Figure 15: LTE-U/WiFi coexistence scenario using different LTE-U channel access mechanisms (a) percentage of lost frames (b) PSNR. 61

Figure 16: Effect of changing the $Txop$ parameter of the modified LBT scheme on the coexistence of LTE-U and WiFi. 61

Figure 17: Effect of changing the GOP size on the LTE-U/WiFi coexistence using the modified LBT scheme. 62

Figure 18: Effect of changing the energy detection threshold of the adaptive p-persistent CSMA scheme on the coexistence of LTE-U and WiFi. 63

Figure 19: Effect of changing the GOP size on the LTE-U/WiFi coexistence using the adaptive p-persistent CSMA scheme. 63

Figure 20: Simulation setup. 77

Figure 21: System model for the QoE-based dynamic channel selection scheme.. 78

Figure 22: QoE-based frame assignment scheme compared to random assignment (a) Percentage of lost frames (b) Average user PSNR (c) Average user delay (d) Average user Jitter. 80

Figure 23: Two WiFi operators coexisting in the same channel (a) Percentage of lost frames (b) Average user PSNR. 83

Figure 24: LTE's performance when the entire video is transmitted over the licensed channel (a) Percentage of lost frames (b) Average user PSNR. 83

List of Tables

Table 1: Mean Opinion Score. 30

Table 2: PSNR to MOS mapping. 31

Table 3: Simulation parameters for the frame type-based channel access. 58

Table 4: List of Notations 66

Table 5: Simulation Parameters for the QoE-based dynamic channel selection scheme. 79

List of Abbreviations

3GPP	3rd Generation Partnership Project
ABS	Almost Blank Subframes
AIFS	Arbitration Inter-Frame Spacing
AP	WiFi Access Point
BER	Bit Error Rate
BLER	Block Error Rate
BSR	Buffer Status Report
CCA	Clear Channel Assessment
CQI	Channel Quality Indicator
CSAT	Carrier-Sensing Adaptive Transmission
CSMA-CA	Carrier Sense Multiple Access with Collision Avoidance
CW	Contention Window
DCF	Distributed Control Function
DIFS	Distributed Inter-Frame Space
E-UTRAN	Evolved UMTS Terrestrial Radio Access Network
eNB	Evolved Node B
EPC	Evolved Packet Core
GOP	Group of Pictures
HeNB	Home eNB
HSS	Home Subscriber Server

ISM	Industrial, Scientific and Medical
LAA	Licensed Assisted Access
LBT	Listen Before Talk
LTE	Long Term Evolution
LTE-A	Long Term Evolution-Advanced
MAC	Media Access Control
MCS	Modulation and Coding Scheme
MME	Mobility Management Entity
MOS	Mean Opinion Score
MSE	Mean Squared Error
OFDM	Orthogonal Frequency Division Multiplexing
OFDMA	Orthogonal Frequency Division Multiple Access
P-GW	Packet Data Network Gateway
PSNR	Peak Signal to Noise Ratio
QAM	Quadrature Amplitude Modulation
QoE	Quality of Experience
QoS	Quality of Service
RB	Resource Block
RBG	Resource Block Group
S-GW	Serving Gateway
SNR	Signal to Noise Ratio
STA	WiFi Station

TBS Transport Block Size

TDD Time Division Duplex

TDM Time-Division Multiplexing

TTI Transmission Time Interval

Txop Transmission Opportunity

U-NII Unlicensed National Information Infrastructure

UE User Equipment

WiFi Wireless Fidelity

Chapter 1: Introduction

Smart handheld devices are increasingly becoming an integral part of people's daily lives. The increasing popularity of multimedia content coupled with the advancements in mobile applications have made these devices indispensable to the majority of the population. This increase in smart device usage has lead to an explosion of data traffic bringing along with it an increasing demand on bandwidth for data. In 2016 alone, Cisco reported a global mobile data traffic growth of 63% reaching 7.2 exabytes of data per month [1]. This growth is expected to increase seven-fold by the end of 2021 as shown in Figure 1 reaching 49 exabytes per month at a compound annual growth rate of 47%.

Having a closer look at the statistics, it is found that 4G connections comprise the majority of the data traffic. In 2016, 4G connections carried 69% of the total mobile traffic. This growth is expected to continue as depicted in Figure 2 where it is expected to reach 79% of the total mobile data traffic by 2021 generating twice as much data on average as a 3G connection.

The continual upsurge of mobile data traffic places great demands on bandwidth for data, especially for 4G connections which are operating in the licensed spectrum. This is the portion of frequencies in the radio spectrum that are regulated by governmental agencies and sold to telecom operator companies for a licensing fee. Each operator is assigned a portion of the spectrum to which it has exclusive access rights without

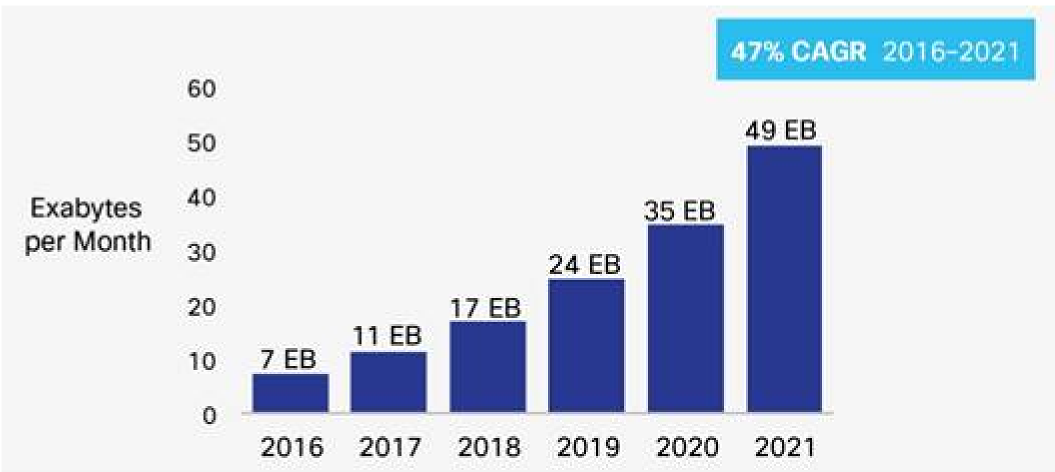

Figure 1: Global mobile data traffic, 2016 to 2021 [1].

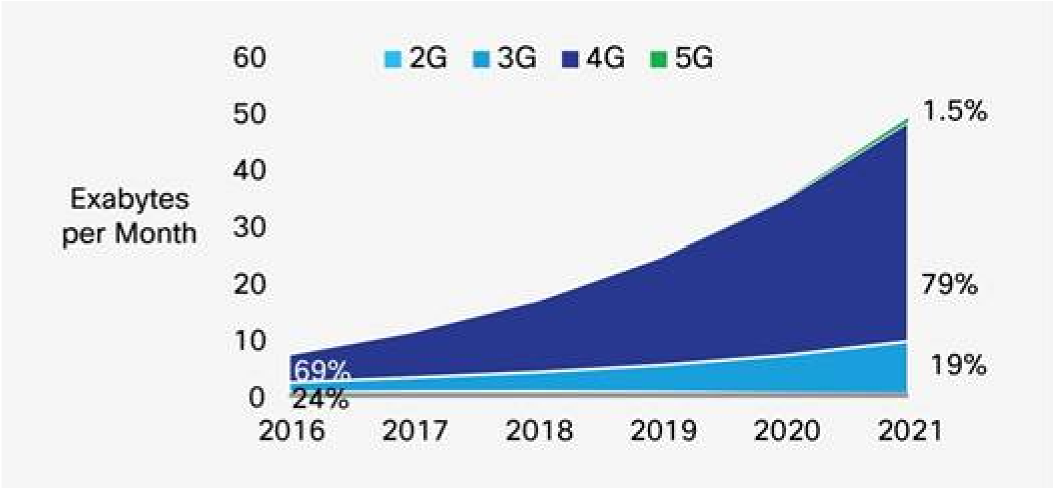

Figure 2: Global mobile data traffic based on connection type [1].

competition from other operators or radio access technologies. The licensed spectrum, however, is a finite resource that is quickly being depleted due to the current huge volume of mobile data with very limited space available to accommodate the expected rise in the upcoming years. This problem, also known as bandwidth scarcity, will lead to many negative consequences including slower services offered to users, increased network congestion, and price inflation [2].

The most common implementation of 4G technology is Long Term Evolution (LTE). Efforts have been made to increase the capacity of LTE networks through multiple means. Media Optimization, traffic offloading and LTE-Advanced are a few examples. Media optimization solutions aim to reduce network congestion by reducing data traffic volumes. These techniques include dynamic adjustment of video bit rates based on bandwidth availability and load time reduction of web pages by pipelining HTTP requests [3]. Traffic offloading is another techniques that aims to relieve congestion in cellular networks by switching over data transmission from cellular networks to other neighboring WiFi networks. This is carried out either in a fully integrated manner where the WiFi network is connected to the cellular core network, or in a partially integrated manner where the users data are moved to the WiFi network whenever they happen to be in WiFi coverage [4], [5]. LTE-Advanced is another technology that is gaining a lot of popularity due to the enhanced network performance that it is offering. It is an extension of LTE that exploits several new technologies such as spatial mutliplexing where multiple antennas are used in parallel to increase the overall bitrate, carrier aggregation where multiple carriers are simultaneously used to expand the bandwidth, and relay nodes which are used to enhance the cell coverage [6].

The most recent proposal has been the extension of LTE operation to the unlicensed spectrum, also know as LTE-Unlicensed. The unlicensed spectrum is the portion of the radio spectrum open to public use for free as long as certified radio equipment are used and technical requirements such as transmission power limits are met [7]. Since all users and technologies have equal access rights to the unlicensed bands, transmissions in these bands are subject to collision and interference. Current radio access technologies operating in the unlicensed spectrum include WiFi, Radar, and Medical Instruments. By aggregating bandwidth from both the licensed and unlicensed spectra, LTE networks can accommodate more users and achieve higher data rates.

The extension of LTE operation to the unlicensed spectrum is carried out through the deployment of dense small cell networks and the use of carrier aggregation with one primary carrier in the licensed spectrum aggregated with one or more secondary carriers in the unlicensed spectrum. Signaling and control messages are communicated the primary carrier while user data is communicated using both the primary and secondary carriers [8], [9], and [10]. Of the many unlicensed bands available, 5GHz bands such as the Industrial, Scientific and Medical (ISM) bands and the Unlicensed National Information Infrastructure (U-NII) bands are found to be the best choice for implementing LTE-U. These underutilized 5 GHz bands have less congestion, a larger amount of available spectrum, a shorter communication range, and limitations on maximum transmit power which makes them very suitable for small cell deployment [9], [10].

LTE-U technology will offer many advantages to current LTE users. The aggregation of both the licensed and unlicensed spectra will create a high boost in the data rates offered by the network. The transmission of the control plane messages over the licensed spectrum will ensure that the users enjoy the higher throughput values offered by the extra bandwidth in the unlicensed spectrum without compromising the reliability and security of their connections. Furthermore, the unified network architecture operating both the licensed and unlicensed spectra will ensure that the users in the unlicensed bands enjoy the same degrees of mobility and coverage available for the users in the licensed bands [9].

One major challenge, however, faces the implementation of LTE-U and that is coexistence with other wireless technologies operating in the same unlicensed band, especially WiFi. The difference in channel access mechanisms adopted by the two technologies prevents fair sharing of the spectrum by both. WiFi adopts a contention-based channel access mechanism where it senses the channel prior to transmission and transmits only if the channel is available. On the other hand, LTE uses a centralized scheduling-based MAC and transmits persistently as long as there is data to be transmitted [11]. This will result in LTE taking over the channel with little or no chance for WiFi to transmit making it subject to great performance degradation.

3GPP release 13 has standardized one form of LTE-U known as License Assisted Access (LAA) for deployment in Europe Japan among other countries, where the use of Listen Before Talk (LBT) is mandatory in the unlicensed spectrum. LBT is a channel access mechanism similar to the one adopted by WiFi where the channel is sensed prior to transmission and only used if found free. The search continues, however, for other channel access mechanisms that are more effective than LBT in achieving a fair coexistence with WiFi while still maintaining high LTE performance.

The focus of this thesis will be on coexistence mechanisms that are most suitable for video transmission. Since looking at statistics, video traffic has accounted for the majority of the data traffic in the last year and will continue to do so in the upcoming years. Figure 3 depicts the increase in mobile video traffic over the period from 2016 to 2021. In 2016, mobile video traffic accounted for 60% of total mobile data traffic. In 2021, this number is expected to rise to 78%, increasing 9-fold and accounting for more than three-fourths of the worlds total data traffic. The dominance of video traffic over other types of traffic is due to the fact that video content has much higher bit rates than other content types hence consuming more bandwidth than other content types [1].

In this thesis, two channel selection schemes for video transmission over LTE-U are proposed. The first is a static channel selection scheme in which the LTE-U UEs are assigned to channels based on their frame type. The second one is an adaptive channel selection scheme that aims to achieve harmonious coexistence with WiFi while

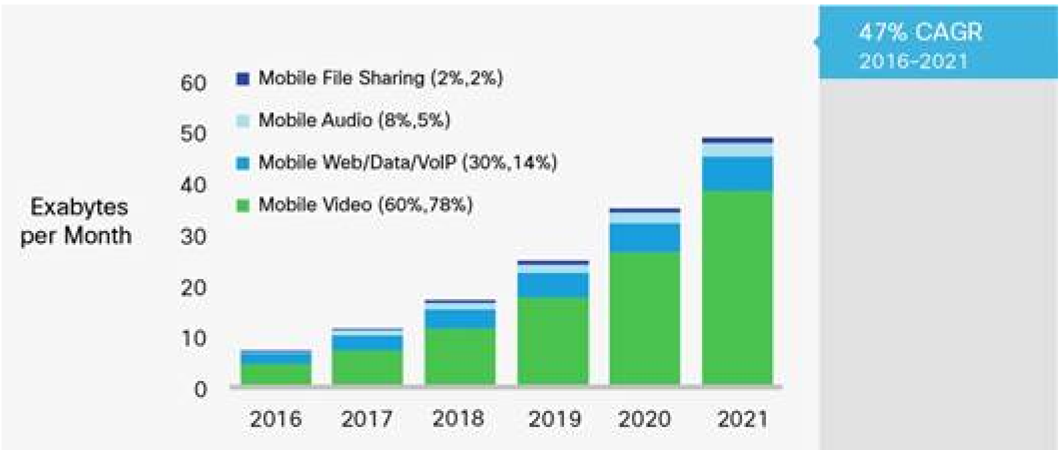

Figure 3: Mobile data traffic breakdown based on content type [1].

jointly taking into account the QoE requirements of the UEs. The UE video frames are dynamically assigned to channels based on three factors: the predicted PSNR, the predicted delay, and the interference caused to WiFi. A framework for predicting the PSNR of a video frame transmitted to a UE taking into account channel fading effects is presented. In addition, based on the historical average of a UEs throughput, another framework for predicting the transmission delay of a frame to that UE is presented. Using these two factors in addition to the probability of causing interference to WiFi, the channel selection problem is formulated as a multi-objective optimization problem with three priority levels whereby the eNB assigns UE frames to different channels with the aim of maximizing the average UE PSNR, minimizing the average frame delay, and minimizing the probability of interference to WiFi.

1.1. Background

This section presents a brief overview on the operation of LTE and WiFi technologies, and some basic background on digital video compression.

1.1.1. LTE

Long Term Evolution (LTE) is a technology that came as an upgrade to the 3G standards. It is the main radio access technology adopted in 4G telecommunication systems today. LTE was first introduced in 2004 by the Third Generation Partnership project (3GPP) and finally standardized in 3GPP's Release 8 in 2010. It combines several new technologies along with a simplified network architecture that allows it to facilitate faster real-time connections outperforming it's 3G predecessor. Peak data rates in LTE networks reach 300 Mbps in the downlink and 75 Mbps in the uplink, latency is limited to 10 ms, and mobility is supported up to 350 km/h [12], [13].

1.1.1.1. Network architecture

LTE is deployed in cell structures with a base station at the centre of each cell covering a radius of 5 to 100 kilometers.The LTE network architecture, illustrated in Figure 4, is a simple one that is composed of three main components: the core network, the Evolved UMTS Terrestrial Radio Access Network (E-UTRAN), and the User Equipment (UE). UEs consist of the devices used by the end users of the network including smart phones and tablets. The E-UTRAN consists of a network of base stations, each known as the evolved Node B (eNB), which are responsible for connecting the end users to the core network. The core network, also known as the Evolved Packet Core (EPC), consists of four main entities: the Mobility Management Entity (MME), the Home Subscriber Server (HSS), the Serving Gateway (S-GW), and the Packet Data Network Gateway (P-GW). The MME is responsible for managing signaling related to mobility and security for network access, and tracking and paging UEs in idle-mode. The HSS is a central database containing all the information about the network subscribers. It also provides other support functions including call setup and user authentication. The PGW and SGW are responsible for routing UE IP packets and connecting the LTE network to other networks such as the internet [14], [13].

1.1.1.2. Physical layer

On the physical layer, LTE employs adaptive modulation and coding where the modulation scheme and the code rate of the forward error correction (FEC) are varied based on the channel condition so as to maintain a maximum throughput. Modulation schemes employed by LTE are QPSK, 16-QAM, and 64-QAM. The FEC scheme used is turbo coding. To combat the effects of channel fading, Orthogonal Frequency Division Multiplexing (OFDM) is used. Instead of modulating the information on a single carrier that spans the bandwidth of the channel, information is modulated on multi-

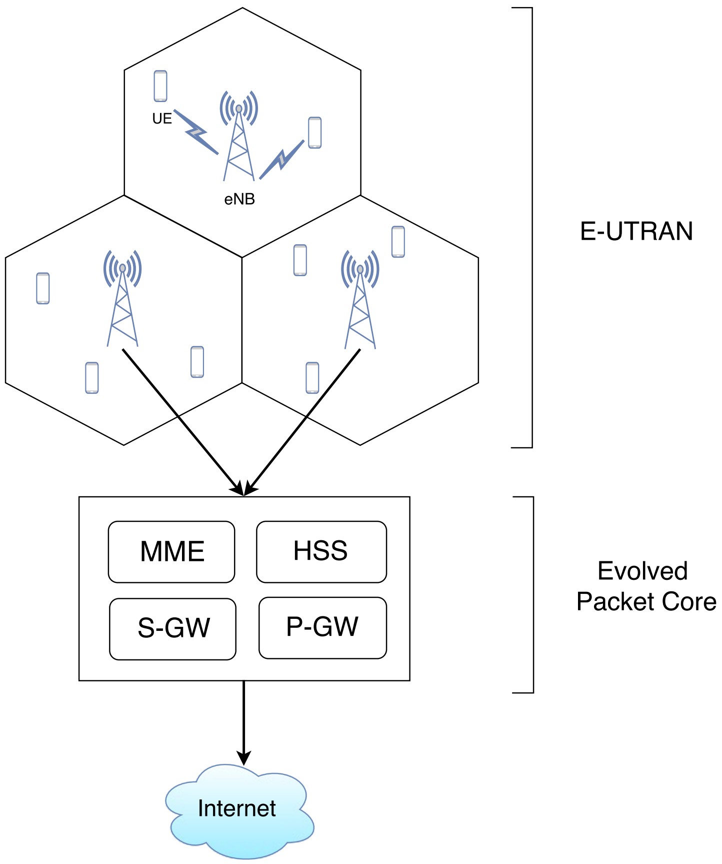

Figure 4: LTE network structure.

ple narrowband orthogonal subcarriers thus transforming the channel from a frequency selective fading channel into multiple smaller flat fading channels.

Uplink and downlink transmissions are managed in one of two ways. The first is Frequency Division Duplex (FDD) where uplink and downlink transmissions occur simultaneously on different frequency bands. The second is Time Division Duplex (TDD) where uplink and downlink transmissions occupy different proportions of time on the same frequency band. Channel bandwidths in LTE are flexible and vary from 1.4 MHz to as wide as 20 MHz. Wide channel bandwidths allow for a boost in the network speed while the flexibility allows for easier migration form legacy technologies such as 3G. Having flexible channel bandwidths also makes the worldwide deployment of LTE easier as the bandwidth can be changed depending on the amount of spectrum available to each operator and the regulatory requirements of each region. LTE also employs Multiple Input Multiple Output (MIMO) technology using multiple parallel antennas to

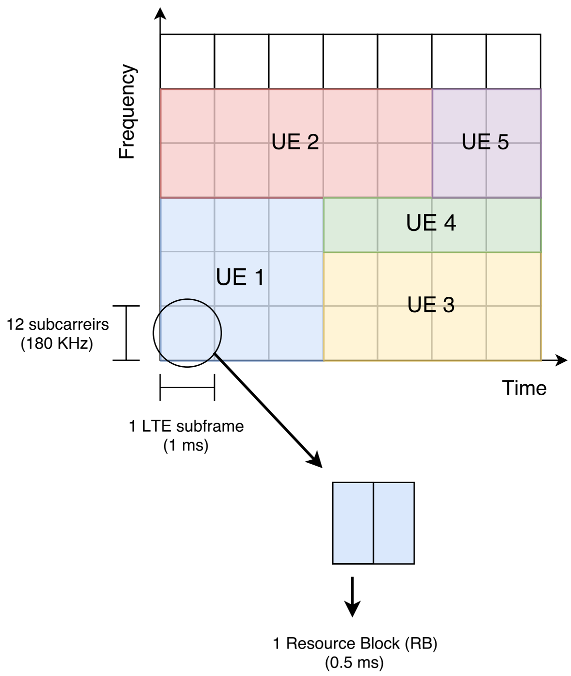

Figure 5: OFDMA: The allocation of time-frequency resources to different UEs.

simultaneously transmit several data streams over the same carrier and hence increase the overall bitrate.

Transmissions in LTE are managed in terms of time units called radio frames. Each LTE frame has a duration of 10 ms and is further divided into smaller units called subframes, each of a duration of 1 ms. A subframe is also called a Transmission Time Interval (TTI). Each subframe consists of two slots of 0.5 ms duration. Channel access in LTE is managed in terms of resource blocks. A Resource Block (RB) is a time-frequency unit assigned to a UE by the eNB for channel access. It has a duration of one slot in time, and is composed of 12 subcarriers in frequency amounting to a total of 180 kHz of bandwidth. Managing transmissions from multiple users is accomplished using Orthogonal Frequency Division Multiple Access (OFDMA). It is an extension of OFDM where data from different users are multiplexed in both the time and frequency domains through the allocation of different resource blocks as shown in Figure 5. The next section further illustrates the details of this process.

1.1.1.3. Scheduling

The allocation of resource blocks to UEs is carried out through a process called scheduling. Each UE can be assigned one or more RBs based on a certain number of factors and the scheduling algorithm employed by the eNB. Upon requesting channel access, the UE supplies the eNB with certain information about the quality of its connection, the nature of the data pending transmission, and the status of its buffer. The eNB, then, decides which RBs to assign to the UE based on the scheduling algorithms that it is using. Scheduling algorithms are operator-specific. Each operator may adopt a different scheduling algorithm than the other. There are, however, some standard scheduling algorithms such as the proportional fair, round Robin, and Best Channel Quality Indicator (CQI). For example, the proportional fair algorithm, takes into account the current achievable rate for each UE and the historical average of the rates achieved by the same UE in the past. It will assign a given RB to the UE that has the largest current-to-average-rate ratio over that RB. The Round Robin Algorithm, on the other hand, assigns RBs to UEs in a token-based fashion, where UEs take turns accessing the channel. Operators may also invent their own scheduling algorithm.

1.1.2. WiFi

WiFi stands for Wireless Fidelity. It is mainly an indoor wireless local area network based on the IEEE 802.11 standards. WiFi is designed to provide indoors wireless connectivity and can cover a distance up to 100 meters with a data rate of up to 54 Mbps. It does not, however, support mobility [13].

The network architecture in WiFi consists of two types of components: Access Points (AP) and stations (STA). Stations are the users mobile devices including laptops, phones, tablets, etc. Access points are the main entities that connect the users to the internet and consist of antennas (for large public spaces) and routes (for homes). WiFi is mainly employed as hot spots as shown in Figure 6 [15] where an access point is connected to the Internet and any wireless device entering the range of the access point can connect to the Internet.

For the physical layer specifications, WiFi operates only in half-duplex mode employing Time Division Duplex (TDD). All stations and access points share the same channel bandwidth. Older WiFi standards supported fixed channel bandwidths, 20MHz for 802.11a/g standards and 25MHz for 802.11b standard. Newer WiFi standards support multiple bandwidth options such as the 802.11n standard that supports both 20 and

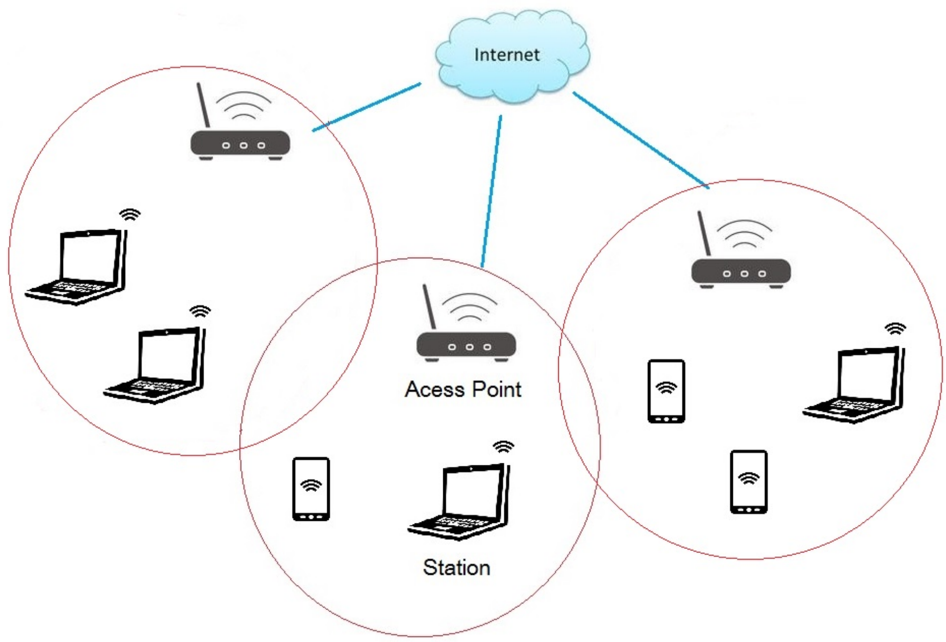

Figure 6: WiFi network structure.

40 MHz operation modes, and the 802.11ac standard the supports 20, 40, and 80 MHz operation modes. All standards operate in the unlicensed portion of the radio spectrum occupying either the 2.4 or 5 GHz bands as is the case with the 802.11a/g/n standards, or operating exclusively in teh 5.8 GHz band as is the case with the 802.11ac standard. All new standards employ OFDM technology and BPSK, QPSK, 16QAM, or 64QAM modulation schemes.

For the MAC layer, WiFi employs a contention based channel access mechanism called Carrier Sense Multiple Access with Collision Avoidance (CSMA/CA). This is a sensing-based channel access mechanism in which the WiFi node only accesses the channel if it is sensed free. Otherwise, it backs off for a random amount of time before sensing the channel again. CSMA/CA is implemented in 802.11 standards using the Distributed Cooridination Function (DCF) Protocol. The operation of the DCF protocol is illustrated in Figure 7 and can be summarized as follows. Prior to transmission the WiFi node performs a clear channel assessment (CCA) whereby it senses the channel for ongoing transmissions for a period of time called the Distributed Inter-Frame Space (DIFS). If the channel is found idle, the WiFi node transmits immediately. Otherwise, a backoff mechanism is invoked. WiFi employs binary exponential backoff wherein a

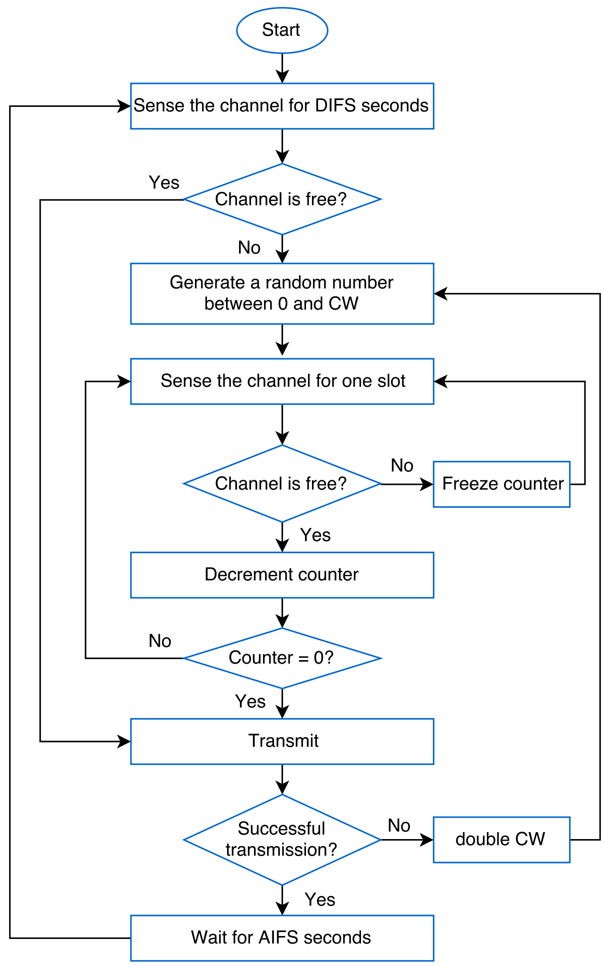

Figure 7: Carrier sense multiple access with collision avoidance.

counter number is generated randomly from the range [0, CW_{min}] where CW_{min} is the minimum contention window. The WiFi node then senses the channel for a sequence of successive time slots, each slot typically lasting 9 μs. If the channel is found to be idle in a slot, the counter is decremented. When the counter reaches 0, the WiFi node transmits immediately. If a collision occurs, the contention window is doubled and the same process is repeated again. Every collision and retransmission attempt is called a backoff stage. After each successful transmission, the contention window is reset to CW_{min} and the WiFi node waits for a period of time called the Arbitration Inter-Frame Spacing (AIFS) before attempting another transmission.

1.1.3. Digital video compression

A video sequence consists of a series of consecutive picture frames displayed at a certain frame rate creating the illusion of motion. Due to the large collective size

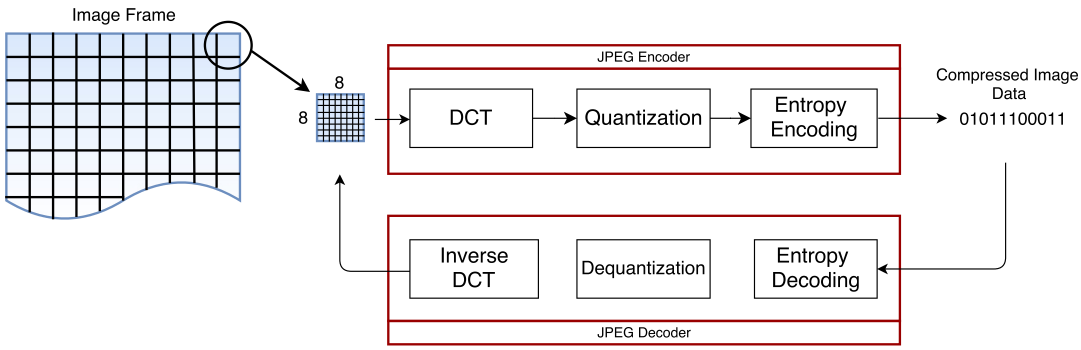

Figure 8: Block diagram for JPEG compression.

of video frames, video sequences are compressed before transmission. Compression reduces the overall size of the video sequence by removing redundancies and irrelevant information. Video compression entails two types, compression of single frames, also known as Intra-frame coding and compression of consecutive frames known as Inter-frame coding.

1.1.3.1. Intra-frame coding

In intra-frame coding, each separate frame is individually compressed. The most popular standard used for this process is JPEG. The JPEG algorithm, illustrated in Figure 8, compresses images through two main processes known as transformation and quantization. Each frame is divided into a set of 8x8 non-overlapping pixel blocks. For each block a Discrete Cosine Transform (DCT) is performed to transform the block to the frequency domain. DCT provides a break down of the frequency components in the block, illustrating how quickly each pixel value is changing. Since changes in high frequencies are least detected by the human perception, the high frequency values in each block are discarded. This is carried out through the next process known as quantization where the frequency coefficients are divided by different scaling factors according to their importance. Lower frequency components are divided by smaller factors to preserve their information while higher frequency components are divided by large factors rendering them close to zero. All coefficients are then rounded to the closest integer. This will result in some degree of information loss that is irreversible thus lowering the picture quality [16].

1.1.3.2. Inter-frame coding

The second form of compression, carried out between consecutive frames, is preformed using a process known as motion estimation and compensation. It aims to remove the temporal redundancies between successive video frames by preserving only the differences between them. In motion estimation, which is the first stage, each video frame is divided into a set of smaller units called macroblocks. For each block, the encoder would search the previous frame for the closest match in terms of pixel value. The closest match is determined based on a distortion measure criteria called the mean absolute difference. It is calculated using the following formula

$$\frac{1}{b^2}\sum_{j=1}^{b}\sum_{i=1}^{b}\left|B_{ij}-C_{ij}\right|, \tag{1}$$

where b is the dimension of the block, B_{ij} is the pixel value of the original block, and C_{ij} is the pixel value of the block under comparison. To mark the position of the best match block, Motion Vectors are used. A Motion Vector (MV) is the difference in the top left coordinates of the two blocks. MVs are coded in a lossless manner as they are used at the decoder to reconstruct compressed frames. In motion compensation, the second stage, a new empty frame is created and filled with the best match blocks positioned at the palace of the original blocks. Then this frame (the motion compensated one) is subtracted from the current frame and the difference frame is encoded. This process is futher illustrated in Figure 9. Frames which undergo this process are called predicted frame or P-frames. In contrast, frames that are not predicted from previous frames are called intra coded frames or I-frames. The most common standard used for this is MPEG. In MPEG, motion estimation can also be carried out in a bidirectional way where both the previous and the following frames are used as a source of prediction and a weighted average of the forward and backward best match locations is used. This results in a third type of frames called Bidirectional frames or B-frames.

In case of transmitting the video over an erroneous channel, where a frame is received with errors, the prediction of frames from previous ones leads to the propagation of these errors across multiple frames at the decoder. This effect is more severe if the error hits the I-frame that was used as the reference. The source of prediction

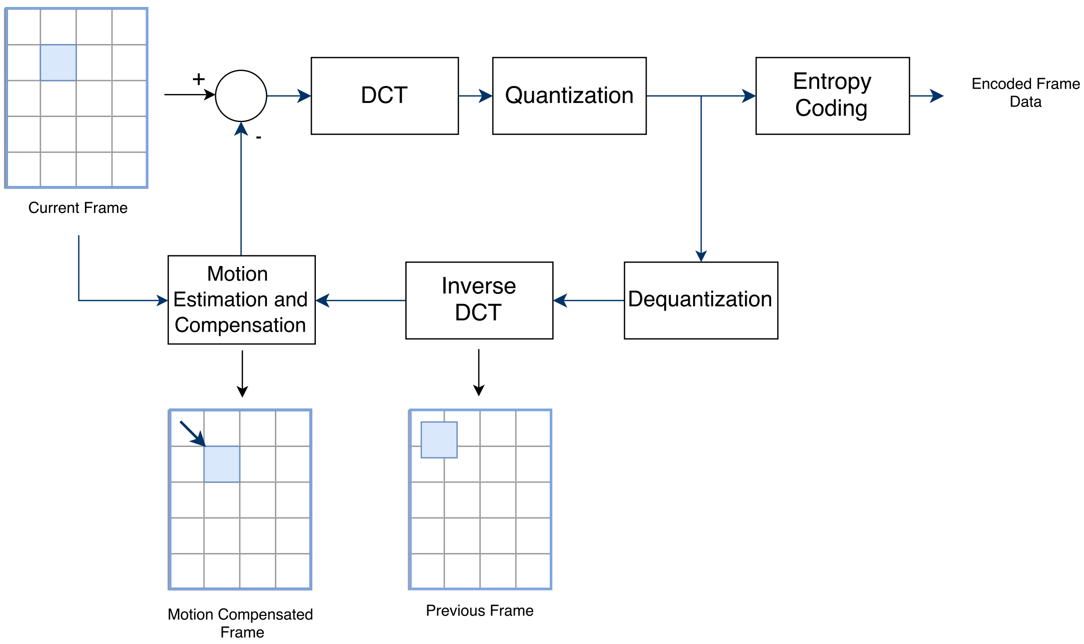

Figure 9: Block diagram for motion estimation and compensation.

at the encoder will then be different from the source of reconstruction at the decoder. Hence, with the addition of each decoded frame, the error accumulates as each decoded frame depends on the frame that precedes it. The decoded video quality also suffers if a P-frame is lost, as the next frame cannot be correctly decoded. To mitigate these problems, periodic I-frames are placed within the video sequence to stop error propagation and provide new references for decoding. This leads to a structure called the group of pictures (GOP). Each GOP begins with an I-frame followed by repeating patterns of P and B frames. One typical GOP structure is shown in Figure 10. The arrows indicate the direction of prediction.

The arrangement of frames in GOP structures leads to two concepts, the coding order and the display order. The coding order, also known as the bitstream order, is the order in which the frames are sent. It is illustrated in Figure 10. Reference frames are sent first, then P-frames, and finally B-frames. The display order is the order in which frames are displayed. It is the same as the original GOP order. For the above example, that would be IBBPBBPBBPBB. The decoding process for the above example can then be summarized as follows. The decoder will first receive the I-frame, decode it, and display it. It will then receive the P-frame, decode it and save it. Following that, it will receive each of the two B-frames, decode, and display them. It will then go back to the

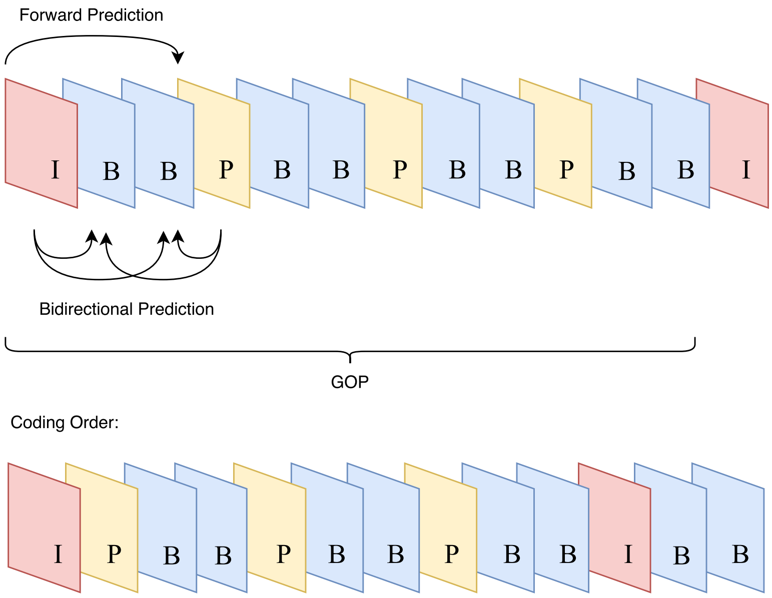

Figure 10: A typical GOP structure.

Table 1: Mean Opinion Score.

MOS	Quality	Impairment
5	Excellent	Imperceptible
4	Good	Perceptible but not annoying
3	Fair	Slightly annoying
2	Poor	Annoying
1	Bad	Very annoying

P-frame and display it. For the next segment, it will receive the P-frame, decode, and save it. Then the B-frames, decode, and display them. Then it will display the P-frame and so on.

1.1.3.3. Video qulaity assessment

The quality of a reconstructed frame can be measured using either subjective or objective methods. In subjective methods, the quality of a frame is assessed by humans. A famous subjective measure is the Mean Opinion Score (MOS) in which a panel of human observers assign a score to the frame based on their perception of its quality. The different quality levels corresponding to the scores are summarized in Table 1 below [17].

Table 2: PSNR to MOS mapping.

PSNR (dB)	MOS
> 37	5 (Excellent)
31 - 37	4 (Good)
25 - 31	3 (Fair)
20 - 25	2 (Poor)
< 20	1 (Bad)

On the other hand, objective measures aim to quantify the frame quality in terms of mathematical models independent of human perception.The most common objective measure is the Peak Signal to Noise Ratio (PSNR). PSNR quantifies the image quality by measuring the similarity between the original and reconstructed images. It does so by taking the average ratio between the maximum possible pixel power and the noise power. The maximum value a pixel can take is 255 since each pixel is represented with 8 bits. Hence the maximum possible pixel power is 255^2. The noise can stem from information loss due to compression and/or errors introduced during transmission and is quantified using a measure called the Mean Squared Error (MSE). MSE takes the average squared difference between the original pixel value and the reconstructed pixel value thus quantifying the error corrupting the frame. It is calculated as follows.

$$\mathrm{MSE} = \frac{1}{mn} \sum_{i=1}^{m} \sum_{j=1}^{n} \left(X_{orig}\left(i,j\right) - X_{rec}\left(i,j\right)\right)^2, \tag{2}$$

where m and n are the dimensions of the frame, X_{org} is the original pixel value, and X_{rec} is the reconstructed pixel value. PSNR is then calculated as

$$\mathrm{PSNR} = 10\log_{10}\left(\frac{255^2}{\mathrm{MSE}}\right). \tag{3}$$

Large PSNR values indicate good image quality and low PSNR values indicate poor image quality. Table 2 below provides the precise breakdown of the values and their MOS equivalent.

Typically, a PSNR value of 30 dB is considered the threshold below which the quality of the image is considered unacceptable. The quality of the video sequence as a whole is measured by taking the average PSNR over all frames [16].

Chapter 2: Literature Review

As mentioned in the previous chapter, the main obstacle with operating LTE in the unlicensed spectrum is fair coexistence with incumbent WiFi systems. Due to the different methods with which each technology accesses the radio channel, WiFi systems will experience severe interference if LTE starts using the unlicensed channel without modifications to its channel access techniques. WiFi employs a contention based channel access mechanism where the decision to access the channel or not is based on detected transmissions in the channel. LTE, on the other hand, employs a scheduling based channel access where nodes are always granted access to the channel when they have data pending transmission. As a consequence, WiFi nodes will always find the channel busy upon detection and will continuously back off which will subject them to severe delays and low throughput.

To combat this problem some regulatory bodies in Europe and Japan have made it mandatory for LTE to use Listen-Before-Talk schemes (LBT) before accessing the unlicensed channel [18]. Similar to WiFi's CSMA/CA, LTE is required to sense the channel before transmission. If the channel is idle, it is allowed to transmit for a certain amount of time, after which it should cease transmission and sense the channel again. However, using this scheme will make provisioning of Quality of Service (QoS) hard to guarantee for LTE users, as LTE's performance will be subject to different delays and interruptions depending on the ongoing WiFi transmissions over the channel.

Several mechanisms have been proposed in the literature for enabling the harmonious coexistence of LTE and WiFi in the unlicensed spectrum without severely impacting the performance of either. These mechanisms can be divided into 5 categories: Modifications to LBT, non-LBT channel access mechanisms, traffic balancing Mechanisms, resource allocation mechanisms, and energy saving-related mechanisms.

2.1. LBT-Based Channel Access Mechanisms

The techniques proposed in the literature that build on LBT mainly focus on three areas: modifying the backoff mechanism of LBT, modifying the sensing process of LBT, and managing the idle time LTE-U spends off the channel post transmission. The main goal of all three being to preserve the continuity of LTE-U transmission as much as possible while also providing maximum transmission opportunities for WiFi.

2.1.1. Modifications to the current LBT back-off mechanism

For back-off mechanisms, some works suggest new backoff designs for LBT such as the one proposed in [19] where the authors propose a modified LBT (MLBT) mechanism where the random backoff is replaced with continuous sensing until finding the channel free. Two sub-mechanisms for channel access are further introduced to ensure the continuity of LTE-U transmission while maintaining fairness with WiFi under different traffic densities. For low traffic, dynamic channel switch (DCS) is used wherein LTE-U switches between different channels to avoid occupying any one channel for a long period of time. For high traffic, where all channels are equally busy, Adaptive Almost Blank subframes (ABS) are used to provide constant transmission opportunities for WiFi. Traffic is measured based on the numbers of LTE-U and WiFi users in the channel which is reported by both to the mobility management entity of the LTE network.

Other works build on current backoff mechanisms of contention-based channel access schemes and mostly focus on the contention window size. The contention window (CW) is the number of time slots a radio access technology spends off the channel in cases of detecting a busy channel or experiencing a collision. Authors in [20] suggest a backoff mechanism for LTE-U LBT based on a modified version of CSMA mechanisms where the CW size of the backoff mechanism is adaptively changed by the LTE-U eNB based on the results of previous transmissions in the channel. They also couple that with medium reservation techniques that allows the eNB to reserve the channel for resolving hidden node problems and modifications to the LTE-U outer loop link adaptation algorithm to better cope with collisions. Authors in [21] replace the conventional binary exponential backoff scheme with a scheme that adaptively adjusts the contention window size based on the available bandwidth in the licensed spectrum and the WiFi traffic load in the unlicensed spectrum. The main goal is to satisfy the QoS requirements of LTE-U users and minimize the probability of collisions for WiFi users. In addition, they propose an admission control strategy that limits the number of served LTE-U UEs so as to limit the collision probability to WiFi users to a certain threshold. On the other hand, authors in [11] propose a fixed CW size rather than an adaptive one. They argue this based on the fact that the Hybrid Automatic Repeat Request (HARQ) mechanism used by LTE does not waste erroneous transmissions, rather it combines them with re-transmissions leading to the target packet error rate of the initial transmission to be set higher. Following a different approach, authors in [22] suggest a fairness-based analytical framework for determining the optimal CW size with the goal of maximizing the total system throughput. The channel access models for LTE-U and WiFi are represented with a one and a two dimensional Markov chains respectively. Using these models, the channel access probabilities for LTE and WiFi are obtained as a function of the CW size. An analytical expression is then developed for the normalized system throughput and used along with the channel access probabilities to obtain the optimal CW size.

2.1.2. Channel sensing schemes

For sensing schemes, authors in [11] discuss the design aspect of the energy detection threshold, and how varying this value affects the performance of each of LTE-U and WiFi. They also propose the use of signal detection instead of mere energy detection to improve the accuracy of the sensing results. Authors in [23] further propose two channel sensing schemes for LTE-U namely, periodic sensing, and persistent sensing. In periodic sensing, the LTE-U node senses the channel for a fraction of a subframe and transmits for the remainder of the subframe. In persistent sensing, the LTE-U node senses the channel for a whole subframe and transmits in the following several subframes. The authors in [24] develop an adaptive p-persistent CSMA scheme for LTE-U to access the unlicensed band. Unlike the previous schemes where the result of sensing directly grants or denies channel access, in adaptive p-persistent CSMA, the LTE-U node keeps sensing the channel until the channel is idle. It then generates a Bernoulli random variable with mean p and transmits only if this random variable is equal to 1. The probability p is adaptively changed based on the channel condition.

The authors in [25] propose an LBT-based channel access mechanism where the sensing times and transmission rate of an LTE-U node is adjusted according to a coexistence criterion which is not degrading the throughput of the WiFi network more than another WiFi node would. Using WiFi interface to listen to the channel, the LTE-U node knows exactly when the WiFi transmission ends and performs sensing only in the following Arbitration Inter-frame Spacing (AIFS) period. Hence, it will never collide with a WiFi station and the total channel airtime will be divided into two orthogonal airtimes. The authors then analytically derive the transmission attempt probability of an LTE-U node that maximizes its airtime while not degrading the average throughput of a WiFi station more than if another WiFi station was added to the network. Similarly, authors in [26] propose an LBT-based scheme where time is divided into cycles, each consisting of a sensing period, an LTE-U transmission period, and a WiFi transmission period. These parameters can be varied in each cycle in order to achieve a certain WiFi protection level. The LTE-U node senses the channel for a certain duration of time. If the channel is sensed free, it generates a random backoff counter to avoid collisions with other LTE-U nodes. When the backoff timer elapses, the LTE-U node immediately broadcasts a reservation signal to reserve the channel until the beginning of the next subframe where it can start transmission. The total duration of the sensing period and backoff timer are designed to be less than the DIFS period, hence the LTE-U node can easily retrieve the channel access after the WiFi transmission period completes. They also develop an analytical model to evaluate the system throughput for both technologies using this scheme.

2.1.3. LTE-U idle times

Another portion of the literature focuses on assigning idle times for LTE-U where it does not access the channel in order to provide transmission opportunities for WiFi. The authors in [8] suggest using an adaptive LBT (ALBT) channel access mechanism where the LTE-U node leaves a certain number of coexistence gaps after transmission that allows other technologies such as WiFi to transmit in. The lengths of these gaps are tuned according to WiFi activities in the channel. The LTE-U node also senses multiple channels at a time and switches between them to avoid occupying any one channel for a long period of time. Thea uthors in [27] further propose a fair LBT algorithm, denoted F-LBT, that aims to allocate the idle period in an LTE frame so as to increase the whole system throughput while still maintaining fairness between LTE-U and WiFi. An analytical model is derived for the system throughput when LTE-U and WiFi coexist in the same channel using a discrete time Markov chain that model the transmission and backoff process of WiFi. Using that model, an analytical expression for the throughput of each technology is developed. The idle period is then determined by defining a reward function that combines the total system throughput with a fairness index between LTE-U and WiFi, and then optimizing it to find the ideal number of subframes.

Other works also combine LBT with other techniques such as the one in [28] where the authors propose a design for a semi-distributed LTE-Unlicensed scheme that combines LBT with the concept ABS. In this scheme, the LTE-U transmission is divided into a duty cycle of 40 subframes. In a portion of this duty cycle, LTE-U will always transmit, and in the other portion it will use LBT. The On/Off periods are decided by the ABS pattern which indicates which frames the LTE-U transmits in and which are silent.

2.2. Non-LBT Channel Access Mechanisms

Alternative coexistence mechanisms to LBT have been proposed in the literature to solve the coexistence issue between LTE-U and WiFi. These mechanisms can be divided into four different categories: time-division multiplexing techniques that aim to fairly divide the channel occupancy time between LTE-U and WiFi, channel selection techniques in which LTE-U transmissions are switched to different channels in order to minimize interference to WiFi, power control techniques that aim to protect WiFi transmissions by adapting the transmission power of LTE-U nodes, and game-based schemes where both radio access technologies develop strategies to compete for channel resources.

2.2.1. Time-division multiplexing techniques

The first group of methods suggested target the division of airtime between LTE-U and WiFi in a TDM fashion so as to provide constant transmission opportunities for WiFi without subjecting LTE-U to large transmission delays. The authors in [29] discuss an algorithm called carrier-sensing adaptive transmission (CSAT). In CSAT, the LTE-U node senses the channel for a long period of time, then defines a duty cycle in which it transmits in a fraction of the cycle and is off in the other to allow other technologies including WiFi to transmit. During the off period LTE-U can sense the channel activity and adaptively adjust its On/Off ratio. Likewise, authors in [30] suggests a similar method called LTE muting where the LTE-U node is silent in N of every 5 subframes. [9] discusses the use of Almost Blank Subframes (ABS), which is already employed in interference coordination in HetNets, to achieve this muting. ABS, first suggested in [31] for use in the unlicensed channel, are subframes within the main LTE frame with subdued transmission power such that no interference is caused to other technologies during those subframes. The authors in [31] suggest modifying the original ABS to eliminate the reference signals so as to provide completely silent transmission gaps for WiFi. Another duty cycle approach is the one mentioned in [32] where the authors propose to achieve proportional fairness between LTE-U and WiFi using a scheme that dynamically adjusts the probability of LTE-U accessing the unlicensed channel and the fraction of time it occupies the channel based on monitored WiFi activities. Those parameters are calculated through the solution to an optimization problem that aims to maximize the throughputs of LTE-U and WiFi.

2.2.2. Channel selection techniques

The second group of techniques suggested aim to switch LTE-U transmissions between different channels to minimize interference caused to WiFi. The authors in [29] discusses the idea of dynamic channel selection where small cells periodically measure the interference in all channels in the band and choose the channel with the least interference to transmit in. If the interference in the channel occupied exceeds a certain threshold, the transmission will switch to another channel with the least interference. The authors in [33] propose another channel selection functionality for LTE-U based on Q-learning in which prior experience is used to decide the most appropriate channel to transmit in. Using this approach, each LTE-U small cell progressively learns to select the channel that provides the best performance - in terms of throughput - based on previous usage of each channel. The authors in [34] propose another channel selection scheme based on the idea that a channel is best when it gives more cell throughput and and better per UE throughput compared to other channels. The proposed algorithm selects a channel from the set of available unlicensed channels such that the cell throughput is maximized and fairness is maintained by achieving good throughput for each UE. The fairness factor is calculated by taking the standard deviation of the CQIs of all UEs over all available channels. A user offloading algorithm is also proposed that offloads the UEs that are getting lesser throughput to the licensed channel. If the average CQI of the current channel gets lower than a certain threshold, the algorithm is triggered again and a different channel is selected.

2.2.3. Power control techniques

The third group of techniques deal with adapting the transmission power of LTE-U nodes to protect WiFi transmissions. The authors in [35] suggest the use of interference-aware LTE uplink power control where LTE eNBs and UEs measure the interference in the channel to estimate the presence and proximity of WiFi nodes and adjust their transmission power accordingly. The amount of reduction is suggested to be according to a fractional compensation of the measured interference. The authors in [36] compare this approach to the use of the ABS and discuss the trade-offs between the two based on the throughputs achieved by each of LTE-U and WiFi. Following a similar approach, authors in [37] proposes a spectrum etiquette protocol for LTE-U in which LTE-U regards WiFi as the primary user with higher priority to transmit. This protocol is based on both LTE-U and WiFi being able to identify the control information of each other and is implemented in two parts. The first part is responsible for decoding the WiFi PHY frames and obtaining their attributes, based on which, the second part adjusts the transmit power of LTE to adapt to the conditions of the unlicensed channel.

2.2.4. Game-based coexistence schemes

The fourth group of techniques are based on game schemes where each of the

LTE-U and WiFi nodes are considered players competing for channel resources. In [38], the authors use the model of a repeated game where the two operators compete over spectrum resources. At each stage of the game, each of the LTE and WiFi operators decide whether to ask for a favor or share a number of subcarriers with the other operator based on the output of a decision tree. The decision tree takes as an input a vector composed of the downlink signal-to-interference-plus-noise-ratio (SINR), the network load condition, and the encourage factor of the operator, and outputs the number of subcarriers to be utilized by the operator. To encourage operators to share resources, an incentive mechanism is proposed where a prize for sharing spectrum resources and a prize for asking for a favor are assigned. An encourage factor is defined for each operator as the accumulation of the above prizes over the past stages of the game. In addition, a threshold for sharing resources and a threshold for asking favors are defined as well. Similarly, authors in [39] propose another game-based channel access mechanism where UEs can access the channel using one of two ways, scheduled access or random access. The UEs are divided into two groups where the first group employs scheduled access and the second employs random access. The resource blocks are grouped into a set of resource batches and also categorized within the same two groups. A utility function is defined for each resource batch as the probability that a UE is able to utilize the resource batch without interference from WiFi. An optimization game is then formed where the players are the resource batches and the actions are whether to change the group they belong to (scheduled or random access) or remain within the same access group with the end objective of maximizing the network utility.

2.2.5. Unified control of LTE-U and WiFi channel access

Alternatively to the above approaches, another proposal exists in the literature to unify the control of the channel access of each of LTE-U and WiFi under one entity. For example, authors in [8] propose the use of coordinated coexistence techniques using virtualized networks and higher level management. By having a single administrative entity controlling the allocation of resources and the access of each system to the channel, both LTE and WiFi networks use the shared information about their transmission and optimize their usage of the channel. Similarly, authors in [40] propose another centralized approach for controlling the channel access of each of LTE and WiFi that is focused on the total human satisfaction instead of the server provider's benefit. Each user can either use the WiFi network for free or the LTE network for a certain price per data unit. Two satisfaction parameters are introduced for the data rates under LTE and WiFi. The coexistence mechanism is implemented by using a centralized cloud server connected to both the LTE BS and WiFi AP that finds the optimal service selection for the each user (to either LTE or WiFi) and the associated spectrum allocation with the goal of maximizing total human satisfaction. Another example is the work presented in [41] where the authors propose a new coexistence mechanism for LTE-U and WiFi in the unlicensed spectrum through the deployment of hyper-access points (HAP) that serve both as an LTE-U base station and a WiFi access point, jointly coordinating the spectrum allocation and interference management for both. A new coexistence mechanism is proposed that embeds LTE-U transmissions within the WiFi MAC protocol by dividing time into non-overlapping transmission periods for LTE-U and WiFi, called the contention free period (CFP) and the contention period (CP) respectively, the lengths of which are decided by the HAP according to the QoS requirements of the users.

2.3. Traffic Balancing

Another approach to facilitating the operation of LTE in the unlicensed spectrum relates to traffic balancing. Traffic balancing handles the coexistence issue between LTE-U and WiFi in terms of the amount of traffic transmitted over the unlicensed spectrum. It aims to divide the LTE traffic between licensed and unlicensed channels in a fashion that guarantees optimal performance for both technologies. Many works in the literature combine traffic balancing algorithms with other techniques to improve the overall performance of the system.

The authors in [42] and [43] combine traffic balancing algorithms with LBT in the unlicensed channel. In [43], the authors propose strategies for balancing the traffic of LTE femtocells, also known as dual-band femtocells, over the licensed and unlicensed channels in the scenario where the femtocells coexist with macrocells in the licensed channel and WiFi in the unlicensed channel. They formulate an optimization problem that aims to maximize the total user satisfaction of both the LTE femtocell and WiFi users while limiting the interference caused to the macrocell users. The solution to the optimization problem is then the optimal transmission strategy in terms of the transmission power of LTE in the licensed band P the optimal channel occupancy time in the unlicensed band T. Similarly in [42], the authors extend the work to cover both dual-band femtocells and integrated femot-WiFi small cells which use a WiFi interface to access the unlicensed channel. They propose an algorithm to dynamically balance the traffic of both types of cells over the licensed and unlicensed bands based on the state of those bands in terms of real time channels, interference, and traffic condition. Similar to [43], they formulate an optimization problem with the decision variables being the transmission power in the licensed channel P and the channel occupancy time in the unlicensed channel T. According to those parameters, the LTE small cell will adjust its transmission such that it occupies the unlicensed band for T seconds and transmits the rest of the traffic over the licensed spectrum at a power P dBm.

In an alternative approach, the authors in [5] present a different form of traffic balancing where the LTE traffic is either transmitted over the unlicensed channel or offloaded to nearby WiFi networks. By combining data offloading with resource sharing in the unlicensed band, the authors develop a hybrid scheme that aims to guarantee an optimal performance for both networks. This is achieved through an optimization problem that finds the maximum number of users to be offloaded to the WiFi network and number of time resources to be occupied in the unlicensed channel with the objective of maximizing the LTE per-user throughput while guaranteeing a minimum per-user throughput for the WiFi network.

2.4. Resource Allocation and Scheduling

Resources in the unlicensed channel can be accessed in a similar or a different fashion than the licensed channel. Taking into account the different nature of the unlicensed channel in terms of delay and other QoS factors, the LTE-U eNB can choose an optimal method of allocating resources to UEs in the unlicensed channel and/or combine resources from both channels via carrier aggregation to achieve the best performance. Some works in the literature cover new scheduling algorithms for LTE in the unlicensed spectrum and suggest optimal ways of aggregating resources from both the licensed and unlicensed channels to achieve maximum throughput while others combine scheduling algorithm with channel access to achieve harmonious coexistence with WiFi.

Starting with scheduling in the unlicensed spectrum, authors in [44] investigate whether scheduling should be used at all in uplink transmissions in the unlicensed spectrum or whether it should be replaced with random access. This question arises due to the hidden terminal problem that arose when both LTE and WiFi share the unlicensed spectrum, and the fact that, in scheduling, each UE is assigned a particular set of radio resources and can only transmit in those. If, upon sensing the channel, those radio resources appear to be occupied, then the UE cannot access the channel and the LTE network suffers a performance degradation. Thus, the authors provide an analytical framework for deciding the optimum uplink channel access method based on the size of the resource pool available for the LTE network in the unlicensed spectrum and the probability of the sensed WiFi interference exceeding the predefined threshold.

In [22], the authors propose a scheduling algorithm for LTE to be used in both the licensed and unlicensed spectra. A utility function is defined for each UE that consists of the product of three factors: a matching factor, a proportional fairness factor, and a delay factor. The matching factor is obtained using grey relational analysis and represents the degree of suitability of the type of user application to the channel used (Licensed or Unlicensed). The proportional fairness factor is defined as the ratio of the instantaneous rate to the average rate achieved by the UE in each resource block. The delay factor varies depending on the application. It is a constant for FTP and VoIP applications and a function of the waiting time of head-of-line packet in the queue of the UE in case of video applications. A linear optimization problem is then formulated that aims to maximize the utilities of all UE by deciding which resource block on which channel to assign to each UE.

In terms of scheduling algorithms specifically designed to achieve a good coexistence with WiFi, the authors in [45] propose a cross-layer proportional fairness-based resource allocation framework for LTE-U that aims to achieve harmonious sharing of the channel by all the LTE-U UEs and WiFi users. The average throughput of each of the LTE-U and WiFi is defined as a function of their channel occupancy time. They formulated an optimization problem that aims to maximize the average user throughput of both systems by finding the optimal ratio of the channel occupancy time of both LTE-U and WiFi, the subcarrier allocation of LTE-U UEs, and the power allocation of each subcarrier. This optimization problem is further decoupled into two sub-problems to reduce the complexity of the solution. To obtain the feasible set ratios of channel occupancy times of LTE-U and WiFi, a Markov model is proposed that analyzes the interaction between the LTE-U and WiFi networks based on the LBT channel access mechanism adopted by LTE-U. Similarly, the authors in [46] formulate the resource allocation of LTE-U in the unlicensed bands as an optimization problem that aims to maximize both LTE-U and WiFi users' throughputs by finding which LTE-U users to allocate to which unlicensed bands. All LTE-U users sharing an unlicensed band are assigned equal shares of time. To simplify the solution to the problem, it is modeled as a student-project allocation matching game where the UEs, unlicensed channels, and eNBs represent the students, projects, and lecturers respectively. Just as lecturers offer projects and students apply for them, eNBs offer available unlicensed bands and UEs apply to use those bands. Using the matching algorithm, eNBs find the optimum set of UE-channel pairs that would satisfy the constraint of the maximum allowed interference to WiFi and the UEs preferences in terms of data rates.

2.5. Additional Aspects of LTE-U Operation

In addition to coexistence with WiFi, some works in the literature have also focused on other aspects of LTE-U operation including multi-operator LTE-U coexistence and energy efficiency improvement. The authors in [47] propose a mechanism for mitigating the inter cell interference caused by multiple LTE-U operators occupying the unlicensed channel when LBT-like access mechanisms are not employed. This mechanism is based on a time-division multiplexing technique where operators negotiate the employment of orthogonal non-overlapping CSAT duty cycles for their transmissions in the unlicensed channel. The negotiation is done over the backhaul X2 eNB signaling interface where small cells exchange relevant information about their transmission and the channel.

In terms of energy consumption, the authors in [48] propose a method to improve the energy efficiency of LTE-U in the unlicensed spectrum when carrier aggregation is used. This is done through the usage of carrier component On/Off scheduling scheme that is based on the idea that some of the channels in the unlicensed band will always be largely occupied which means that the probability of LTE-U to accessing them will be very small. Therefore, to save the energy that would otherwise be wasted on monitoring and waiting for the channel, that channel would be turned off. The authors in [42] further present a method for selecting which carriers to turn off that would results in a good compromise between energy consumption and throughput.

2.6. Surveys and Comparative Studies of Different Coexistence Mechanisms

Other works in the literature focus on evaluating and comparing different coexistence mechanism developed for LTE-U. The authors in [9], [36], [49], and [50] all survey the technical challenges facing the implementation of LTE-U and discuss the main implementation aspects and technologies developed for enabling LTE-U/WiFi coexistence. The authors in [49] specifically overview two main time-sharing coexistence mechanisms namely, CSAT and LBT. They compare the two schemes in terms of conforming to current regulatory restrictions, changes required to the LTE standards, and deployment time. They also discuss the design aspects of the two mechanisms and the trade-offs between them. They present simulation results that compare the performance of both and the effect of the design parameters of each, and provide implementation recommendations based on those results.

The authors in [51] further develop a framework for studying the performance of the main coexistence schemes proposed in the literature, identifying the effects of their key design parameters on the coexistence performance. They also develop a throughput and interference model for the LTE-WiFi coexistence that takes into account those parameters. Through extensive simulations, they also investigate the effect of interference coupling among the devices and evaluate which coexistence scheme performs better in different interference coupling scenarios.

2.7. Video Transmission Over Cellular Networks

The last section of the literature review is going to cover video transmission over wireless networks. While there is very little work on video transmission over LTE-U, a vast body of literature addresses video transmission over cellular networks. There are many aspects to video transmission over wireless networks, some of the ones covered here include LTE resource allocation models, scalable video coding transmission, cross layer designs that jointly consider parameters of the physical layer and video application, analytical frameworks for predicting errors and evaluating error control techniques, and modifications to network architecture designs to better suit video transmission.

2.7.1. Resource allocation and scheduling algorithms

Many resource allocation algorithms have been proposed for LTE that are specifically designed for video transmission. These algorithms aim to improve different aspects of the video transmission process such as reducing transmission delays and improving the received video quality. The authors in [52] propose a delay-based bandwidth allocation scheme for HTTP-based video streaming over LTE networks that takes into account both the QoE requirements of each user and the quality of their channels. They propose a Dynamic Minimum Average Delay (D-MAD) scheme that allocates bandwidth on a video chunk basis with the aim of minimizing transmission delays experienced by the users. The bandwidth requested by each user is calculated as a function of the video chunk size, the experienced channel quality level, and the protocol overhead. The users are then collectively allocated portions of the available bandwidth based on the solution to an optimization problem that aims to minimize the average users' chunk delays. Focusing on another aspect, the authors in [53] propose a scheduling algorithm for video streaming over LTE that aims to improve the user perceived video quality. The algorithm takes into account 3 factors: the system throughput, the QoS delay constraints, and the scheduling fairness among UEs. For each UE a weight vector is constructed in which each element corresponds to the weighted combinations of the above factors over one resource block. The UEs are then assigned to the RBs over which they have the maximum weight.

The authors in [54] analytically derive the probability of timely delivery of HTTP streamed video packets as a function of the bandwidth allocated to the user. The model incorporates parameters such as the video chunk size, video chunk play-out time, the ration of the throughput to the actual data link rate (due to added over head at the lower layers), and the spectral efficiency of the users calculated using their CQIs.The attained closed form expression can then be used to calculate the bandwidth that should be allocated to maintain timely video delivery or the number of users that can be accommodated within a certain bandwidth and QoS requirements.

2.7.2. SVC video transmission

Some works in the literature focus on the multilayer nature of the SVC videos and base their approaches on solutions that take those layers into account. The authors in [55] and [56] propose a scheme for the transmission of SVC coded videos over VANETS and wireless mesh networks by selecting the most appropriate path for each layer in the video using Grey Relational Analysis (GRA). The objective is to send the base layer (which is the most important layer) on the best path, the first enhancement layer on the next best path and so on. A set of network parameters consisting of the normalized delay, jitter, loss rate, and throughput for each path is constructed and the Grey Relational Coefficient (GRC) is calculated for each. The base layer is then assigned to the path with the highest GRC, the first enhancement layer to the path with the next highest GRC and so on. Similarly, the authors in [57] propose a distribution algorithm for SVC video streaming over heterogeneous networks in which the best network to stream the video over is selected based on Variance Coefficient Weighting (VCM) and Modified GRA. The matching between a set of video streams to be transmitted and a set of available networks is based on a set of parameters including bandwidth, time delay, BER, etc. A weight is assigned to each network parameter using VCM which is used by the Modified GRA to determine the best network for each bit stream.

In terms of resource allocation for SVC coded videos, the authors in [58] discuss a radio resource management (RRM) scheme for multicast SVC video transmission over LTE based on a sub-grouping technique where the group of UEs interested in receiving the same video are divided into subgroups. The UEs in each subgroup receive the same number of layers based on their perceived channel quality. The resource allocation procedure is done in a frequency selective manner where the UEs are assigned to the resource block in which they experience the highest channel quality and is carried over 2 stages. In the first stage all UEs are allocated enough resources for the transmission of the base layer. In the second stage, based on the CQI measurements received from the UEs, subgroups are formed based on the objective of guaranteeing the highest intra-group spectral efficiency. The subgroups are reconfigured every scheduling frame. The authors in [59] propose another resource allocation framework for SVC video streaming over LTE networks with the aim of maintaining a minimum QoE level for all users at all times. This scheduler, denoted the Three Level Scheduler, works by adjusting the number of enhancement layers and thus the transmission data rates to adapt during different network load conditions while ensuring that the aggregate video quality is maximized and the total number of quality switches is minimized. Two heuristics are developed to accomplish this task, namely the Water-Filling Heuristic and the Balanced Water-Filling Heuristic. They work by increasing or decreasing the number of enhancement layers during changing network conditions such that the aggregate QoE gets minimally degraded or maximally enhanced. The authors in [60] propose a QoE-based Video Delivery scheme over LTE that divides the SVC video layers into QoE-based priority classes based on the quality contribution and bitrate of each video layer. The algorithm assigns the most important priority class to the layers having high video quality contribution while simultaneously having a low bitrate. Marked packets of each flow are stored in subqueues at the eNB, each subqueue representing a priority class. The proposed scheduler works by first selecting the head of line packet from the highest priority subqueue of each flow and then calculating a scheduling metric for each flow based on the exponential proportional fair algorithm(EXP/PF) which is modified to take the QoE priority classes into account. The PRB is assigned to the flow that maximizes the scheduling metric.

2.7.3. Cross layer designs

Cross layer designs focus on jointly adjusting parameters of the application layer and other layers such as the physical or MAC layer to optimize the performance of the video transmission system. The authors in [53] propose a cross-layer system design for optimal real-time video delivery over LTE networks. The objective of the system is to minimize expected video distortion under given packet delay constraints and channel condition. The expected video distortion is calculated using the ROPE method in [61] and the delay constraint is represented by dividing the data bitrate by the bandwidth. A distortion-delay optimization problem is then formulated with the objective of finding the optimal MCS and video encoding parameters such as the quantization step size to minimize the expected video distortion. The authors in [62] propose a multicast video transmission scheme in multi-rate wireless networks. The scheme decides which frame to transmit in a GOP and at which bit rate in order to maximize the perceived visual quality at the users side. The frame- and bitrate-selection problem is formulated as integer programming problem that aims to maximize the PSNR of the received video and is solved using a heuristic called the Marginal-Utility-Based Streaming algorithm. The algorithm greedily selects the frame and bit rate in each iteration that maximize the total utility of frames for all users in all multicast groups.

2.7.4. Analytical models for error control techniques and received video quality

In terms of analytically assessing system performance, the authors in [63] derive a complete analytical model for evaluating the mean squared error of a received H.263 video transmitted over a lossy channel. The model covers the three aspects of video transmission: the encoder, bursty transmission channel, and the decoder. It also takes into account the effects of spatial loop filtering, forward error correction, and inter-frame error propagation at the decoder. Models for the distortion-rate performance of the encoder, the distortion at the decoder and the residual word error rate over the channel are developed. In addition, the transmission channel is modeled using a 2-state Markov model describing burst errors on the symbol level. Using this framework ,the optimal percentage of intra coded macroblocks and the optimal FEC code rate are determined to achieve optimal performance. The authors in [64] propose an analytical framework for the study of error control techniques for video transmission over wireless networks. The focus is on retrasnmission-based error control techniques such as the hybrid automatic repeat request. Two Markov models are used for this process. The first one jointly models the video packet generation and the wireless channel. The second one models the error control process. The framework analyzes the behavior of error control techniques and evaluates their performance in a variety of scenarios.

2.7.5. Video delivery architectures

From an architectural perspective, the authors in [65] propose a proximity-based video delivery architecture for LTE networks that reduces the load on video servers and core network. Instead of going through the EPC all the way to the video server to be sent again, the video packets are rerouted directly from the nearest network node (the eNB or SAE-GW) that is common between the video source and receivers. For example, if both the sending and receiving UEs are in the same cell, the video packets are sent from the first UE to the eNB which then resends to the receiving UE. The resulting load reduction on the core network significantly improves the video packet latency, jitter, throughput, and cell capacity.

The authors in [66] design and implement a cooperative video streaming architecture that combines existing LTE architecture with Device-to-Device (D2D) techniques in order to increase the network capacity and accommodate as many video requests as possible. In crowded scenarios where multiple users request the same video, one copy of the video is downloaded and then shared among the users using their Device-to-Device network. Of the many available D2D techniques, WiFi Direct is chosen due to its numerous advantages in terms of its availability, ease of implementation, and lack of interference with cellular network channels. The group of users is managed using a designated group owner (GO) that assigned the responsibility of managing and controlling the group. The aggregate capacity of all the users' cellular channels is used hence reducing the traffic cost of each device and increasing the overall download speed.

With the plethora of work available covering video transmission over LTE networks, not many exist that cover video transmission over LTE-U. Only the authors in [67] propose a scheme for video transmission over LTE-U based on adaptively assigning video frames to a number of available channels with the aim of maintaining continuous video playback at the receiver. The frame assignment problem is formulated as an optimization problem that aims to maximize the probability of correct reception of video frames. The optimization problem takes four factors into account, namely, the quality of the UE's channel, the WiFi activity on the unlicensed channel, the status of the UE playback buffer, and the deadline and priority of each video frame. Based on the solution of the optimization problem the Home eNB decides which UE to serve and which channel to transmit the UE's frame over.

Chapter 3: Frame Type-Based Channel Access

In this thesis, the focus is on utilizing LTE-U technology specifically for video transmission applications. In addition to the coexistence issue with WiFi, wireless video streaming poses additional challenges on the LTE-U system design due the stringent QoE demands associated with video delivery. The time-sensitive nature of the data being transmitted places strict upper bounds on the delays allowed between two consecutive frames so as to maintain continuous playback at the receiver. In addition, the frames in the encoded video file vary in importance and the loss of different types of frames affect the decoding process differently.

As illustrated in Chapter 2, several channel access mechanisms for enabling the coexistence of LTE-U with WiFi have been proposed in the literature. However, very few addressed the problem of video transmission over LTE-U. Therefore, this thesis further explores the design of efficient LTE-U channel access mechanisms from the perspective of video streaming. Specifically, we propose two channel selection schemes for video transmission over LTE-U. The first is a static channel selection scheme in which the LTE-U UEs are assigned to channels based on their frame type. The second one is an adaptive channel selection scheme in which UE frames are assigned to channels based on the solution to an optimization problem that takes into account the UE's Quality of Experience (QoE) requirements while striving to minimize the interference caused to WiFi. This chapter discusses the static frame type-based channel selection, while the dynamic QoE-based channel selection is covered in more detail in Chapter 4.

3.1. Proposed Approach

The frame type-based channel selection scheme proposed in this chapter takes advantage of the varying sensitivity of the information in an encoded video sequence and the varying characteristics of the licensed and unlicensed channels to distribute that information in an optimal way over the two channels.

As described in Chapter 1, due to the use of motion estimation and compensation when encoding a video sequence, different frame types in a GOP structure vary in terms of their importance for the decoding process. The loss of each frame type affects the received video quality differently. The I-frames are the most important ones for the decoding process. They are the reference frames used as the source of prediction for the other frames in the GOP. The loss of an I frame will mean that the rest of the frames in the GOP cannot be correctly decoded. The P- and B-frames, on the other hand, are the least important ones for the decoding process. They are predicted from previous frames and carry less information than I-frames. The loss of a P-frame, while still affecting the received video quality, will not degrade it as much as the loss of an I-frame would do.

The licensed and unlicensed spectra also exhibit different characteristics which can be utilized to send different types of frames to improve the efficiency of the overall process. The licensed spectrum is regulated by authorities where each operator has exclusive access to its own portion of bandwidth. As a result, it is more reliable, secure, and with guaranteed QoS. However, the amount of available bandwidth there is limited. On the other hand, the unlicensed spectrum has a large amount of available bandwidth, but is open for multiple other technologies to use and access to it is contention based. QoS, therefore, is not guaranteed as transmissions from different users may be subject to collisions and interference.

Taking all that into account, the approach proposed here is to divide the frames of the video sequence over the licensed and unlicensed channels based on their significance and the amount of bandwidth they consume. The I-frames are less frequent throughout the video sequence but are of higher importance for the decoding process. Hence, the are most suitable to be sent over the licensed channel, where limited bandwidth is available but channel access and quality of service are guaranteed. P and B frames on the other hand, are more frequent throughout the video but less significant for the decoding process. Hence, those frames are transmitted over the unlicensed channel where more bandwidth is available but some form of competition with WiFi exists and hence channel access and successful transmission are not guaranteed at all times. Using this scheme, more space is freed up in the licensed channel by sending the bulk of the video sequence over the unlicensed channel. At the same time, the quality of the received video is not compromised as the most important information is sent over the licensed channel.

As mentioned in Chapter 1, 3GPP has mandated the use of LBT as the channel access mechanism for LTE when accessing the unlicensed bands in order to prevent severe interference with WiFi. However, the LBT version proposed by 3GPP is very similar to the CSMA/CA employed by WiFi in terms of the sensing and backoff mechanisms. The problem with using this version of LBT is that it does not provide guaranteed quality of service for LTE users and is very similar to employing WiFi technology through LTE equipment. Therefore, in order to improve LTE's performance in the unlicensed spectrum while still maintaining a harmonious coexistence with WiFi, we couple the above scheme with two time-sharing channel access mechanisms that have been proven to outperform legacy LBT. We compare their performances and test the effect of varying the key design parameters of each on the LTE-U/WiFi coexistence. We additionally experiment with different GOP structures of the transmitted video and note the effect on the received video quality using each of those channel access mechanisms.

3.1.1. Modified LBT channel access

The first coexistence mechanism considered is a modified version of LBT with two main differences to conventional LBT. Firstly, the backoff duration is fixed. Secondly, the sensing duration is extended to multiples of the LTE subframe duration. The channel sensing scheme used is a similar one to the persistent sensing scheme proposed in [23] with the minor modification of extending the sensing duration to 2 ms (2 LTE subframes). The operation of this channel access mechanism is summarized as follows. The LTE-U eNB senses the channel for a duration of 2 ms. If the channel is free, the eNB will transmit for a fixed period of time called the transmission opportunity (Txop). To simplify the needed modifications to the existing LTE architecture, Txop is chosen to be a multiple of the LTE subframe duration. After Txop seconds have elapsed, the eNB halts transmission and repeats the sensing procedure. Figure 11 further illustrates this. By halting transmission at the end of the transmission period and sensing the channel for 2 subframes, LTE leaves several gaps for WiFi to transmit in and hence, prevents bandwidth starvation for WiFi users.

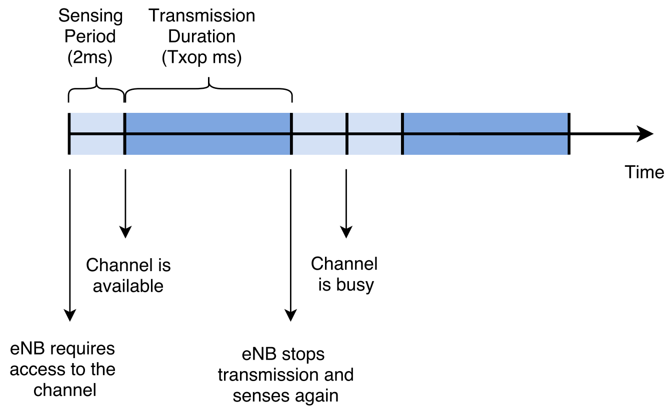

Figure 11: Modified LBT channel access mechanism.

3.1.2. Adaptive p-persistent CSMA channel access

The second channel access mechanism considered is the adaptive p-persistent CSMA proposed in [24]. Conventional p-persistent CSMA uses a probabilistic approach when accessing the channel. Prior to transmission, the interference level in the channel is sensed. If the detected interference is found to be below a predetermined threshold I_{th}, a Bernoulli random variable is generated with probability of success p. If this random variable is equal to 1, the channel is accessed. Otherwise, transmission is deferred to the next time slot. The adaptive p-persistent CSMA proposed in [24] is a modified version of this where the probability of success of the Bernoulli random variable is adaptively changed based on the sensed interference level in the unlicensed spectrum. This ensures that the probability of LTE-U accessing the channel is low when WiFi is most likely to be transmitting, thus avoiding collisions. The measured interference power in the channel I is modeled as a normal random variable with mean I_{mean} and variance σ_I^2. p is then calculated as the tail probability of the standard normal distribution, viz.,

$$p = \frac{1}{\sigma_I \sqrt{2\pi}} \int_I^{\infty} e^{-\frac{(x-I_{mean})^2}{2\sigma_I^2}} dx = Q\left(\frac{I - I_{mean}}{\sigma_I}\right), \tag{4}$$

where I is the interference power in dBm measured by the eNB in the unlicensed channel and $Q(\cdot)$ is the Q-function. The mean and standard deviation of the normal distribution in the above equation are design parameters used to control the shape of the distribution. By varying those two parameters, different WiFi protection levels can be

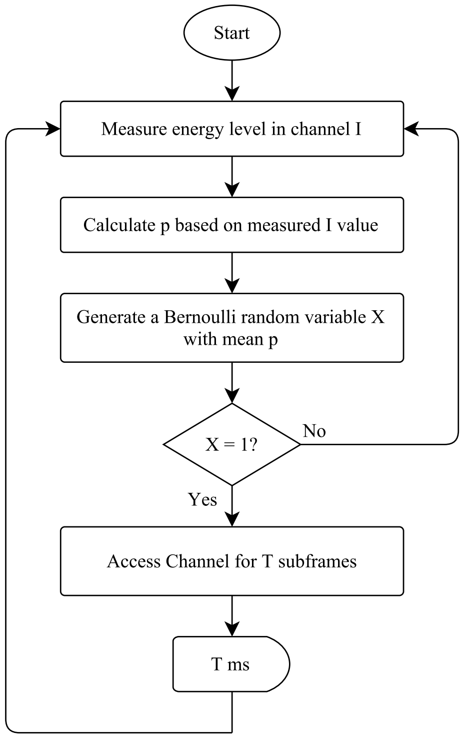

Figure 12: Flow chart for the adaptive p-persistent CSMA channel access.

achieved. A narrow distribution where the mean equals the energy detection threshold is preferred to ensure that the probability of LTE accessing the channel is high when the sensed interference is below the energy detection threshold and low when the sensed interference is above the energy detection threshold. Using this scheme, the eNB first senses the channel and calculates p based on the interference detection results. It then generates a Bernoulli random variable with mean p. If this random variable equals 1, it accesses the channel. Otherwise, it defers transmission to the next time slot. This process is illustrated in Figure 12. Differently from [24], we simplify any needed modifications to the existing LTE architecture by disabling signal detection only using energy detection for calculating the interference level in the channel. In addition, we take the duration of the time slots to be 1 ms, which is the duration of one LTE subframe. The way p is calculated here reflects the WiFi activities in the channel. A large value of p indicates that the channel is most likely to be free while a small value of p indicates that the channel is probably busy.

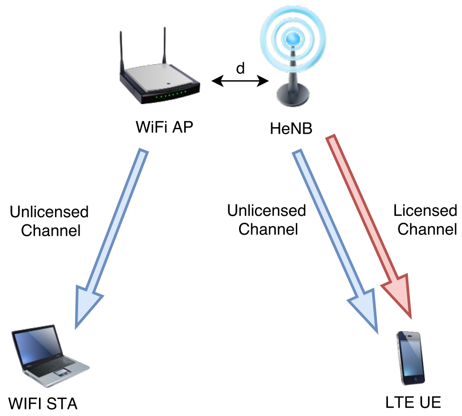

Figure 13: System model for the frame type-based channel access.

3.2. Performance Evaluation

In this section, we present simulation results for the proposed channel access mechanisms and study their impact on the performance of both the LTE and WiFi users. The simulations were conducted using an integration of NS-3 and evalvid softwares.

3.2.1. Simulation scenario

As shown in Figure 13, we consider an indoor simulation scenario where an LTE and a WiFi small cell coexist in the same building with a separation of d m. The number of cells and the node layout are the same as the ones outlined in 3GPP's TR36.889 study [68]. The LTE cell consists of a home e-Node B (HeNB) operating in both the licensed and unlicensed bands serving N user equipment (UEs) while the WiFi cell consists of a WiFi access point (AP) and N WiFi stations (STAs). The WiFi AP operates over the same unlicensed channel as the HeNB with the same center frequency. The N users of each cell are moving randomly within the area. Control and signaling information as well as uplink data of LTE are communicated over the licensed spectrum while the downlink data is communicated over both the licensed and unlicensed spectra according to the schemes discussed in Section 3.1. A remote server is sending a video sequence to each of the $2N$ users through the LTE HeNBs as well as the WiFi APs. All video files are compressed before transmission to reduce the file size.

The scheduler used in the simulation is a proportional fair one. The propagation model used is the ITU indoor propagation model [69]. The remaining simulation pa-

Table 3: Simulation parameters for the frame type-based channel access.

Parameter	Value
Number of cells	4
Channel BW	20 MHz
Center frequency of licensed channel	2.12 GHz
Center frequency of unlicensed channel	5.18 GHz
eNB/AP power	18 dBm
UE/STA power	18 dBm
UE noise figure	9 dB
WiFi standard	802.11n
Speration of AP and HenB	5 m
Channel model	ITU indoor propagation model
Speed of UEs	3 km/h
Antenna type	Isotropic
LTE scheduler	Proportional fair
LTE resource allocation type	Type 0

rameters are summarized in Table 3. The video file used is the "Foreman" test sequence and is encoded using an MPEG-4 codec at a bit rate of 2 Mbps. The resolution of the sequence is 352×288 and it consists of 300 frames with a total duration of 10 seconds. As mentioned earlier, we divide the frames between the unlicensed and licensed channels based on the importance of each frame type. Thus, the encoded video is split into two files, one containing all the I and P frames in the video and is sent over the LTE licensed channel. The other contains all the B frames and is sent over the unlicensed channel. The video is then reconstructed at the UE/STA using the frame index that is sent in each packet header.

3.2.2. Simulation results

To evaluate the performance of the system, two performance metrics are used. These are the average PSNR of the received videos and the average frame loss rate per user. For comparison purposes, simulations were first run for the case where LTE operates only in the licensed channel to demonstrate the spectrum crunch that results from increasing the number of UEs. The results are shown in Figure 14. It can be

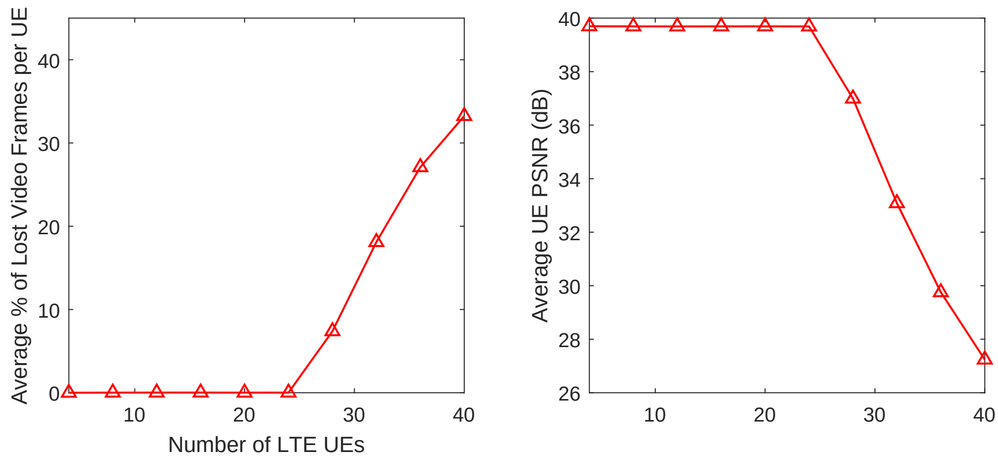

Figure 14: Spectrum crunch resulting from increasing the number of LTE UEs in the licensed spectrum.

noticed that as the number of LTE UEs increases, the quality of the received video starts to degrade and the number of lost frames increases. This is attributed to the fact that a limited number of resources is available for LTE in the licensed spectrum. During each 1 ms period, which is the scheduling interval in LTE-U systems, a certain number of resource blocks is available in the channel that can be allocated to UEs. That number depends on the channel bandwidth. In our simulations a 20 MHz channel was used which corresponds to a 100 resource blocks. In addition, the eNB employs Type 0 resource allocation where every 4 resource blocks are grouped together and assigned to a single UE. That limits the number of UEs that can be served in each 1 ms period to 25 UEs only. If more UEs are present in the channel, the rest may be subject to frame losses. This confirms the need to expand the bandwidth of LTE into the unlicensed spectrum to accomodate a larger number of users who are all requesting video files at the same time.

We now investigate the channel access mechanisms described in Section 3.1 along with the proposed splitting of the video frames between the licensed and unlicensed channels based on the frame type as explained earlier. We simulate each of the channel access mechanisms for different numbers of LTE UEs (4 to 40) while keeping the number of WiFi users constant at 20. We also simulate the scenario where the LTE HeNBs transmit the videos entirely over the unlicensed channel using conventional LBT as a reference access mechanism. The results are shown in Figure 15. The results show that, for all access mechanisms, as the number of LTE UEs occupying the unlicensed channel increases, the performance of WiFi starts to degrade in terms of both the percentage of lost frames as well as the average user PSNR. This is intuitive as the channel is occupied for a longer period of time due to the increasing number of LTE UEs accessing it and the WiFi APs find less and less opportunities to transmit and hence, miss certain frame deadlines leading to a large number of lost frames and low PSNR. However, the damage to WiFi is decreased through using the two proposed access mechanisms in this paper with the p-persistent CSMA channel access mechanism having an edge over the modified LBT. This is attributed to a better accommodation of WiFi by LTE through calculating its probability of accessing the unlicensed channel according to the measured WiFi activities and hence reducing the likelihood of collisions. In terms of the LTE-U performance, it can be seen that the modified LBT and the p-persistent CSMA achieve a comparable performance while both exhibiting a minor performance degradation compared to conventional LBT.

Next, for the modified LBT scheme, we test the effect of the LTE-U transmission duration on the overall performance of both LTE-U and WiFi. We run the simulations for three different values of $Txop$ and observe its effect on the received video quality and frame loss rate experienced by both the LTE-U and WiFi users. The results are illustrated in Figure 16. It is clearly seen that as $Txop$ increases, the performance of WiFi degrades both in terms of the number of lost frames and the average user PSNR while that of LTE-U improves. This is due to the fact that LTE occupies the unlicensed channel for a longer period of time leaving very short transmission opportunities for WiFi. Next, the number of LTE and WiFi users were fixed to 20 each and $Txop$ was fixed to 4 ms. Different GOP sizes of the video were then tested to study their effect on the quality of the video received by the users and the results are illustrated in Figure 17. We notice that when the GOP length was changed from 12 (I B B P) to 16 (I B B B P), the losses for LTE increased as the number of frames transmitted over the unlicensed channel increased. Moreover, the quality of the received video by the LTE UEs decreased since the I and P frames, which are the most important for the decoding process, became less frequent throughout the video sequence. For the case where the GOP length is 30 (an I frame followed by 29 P frames), the losses in WiFi increase

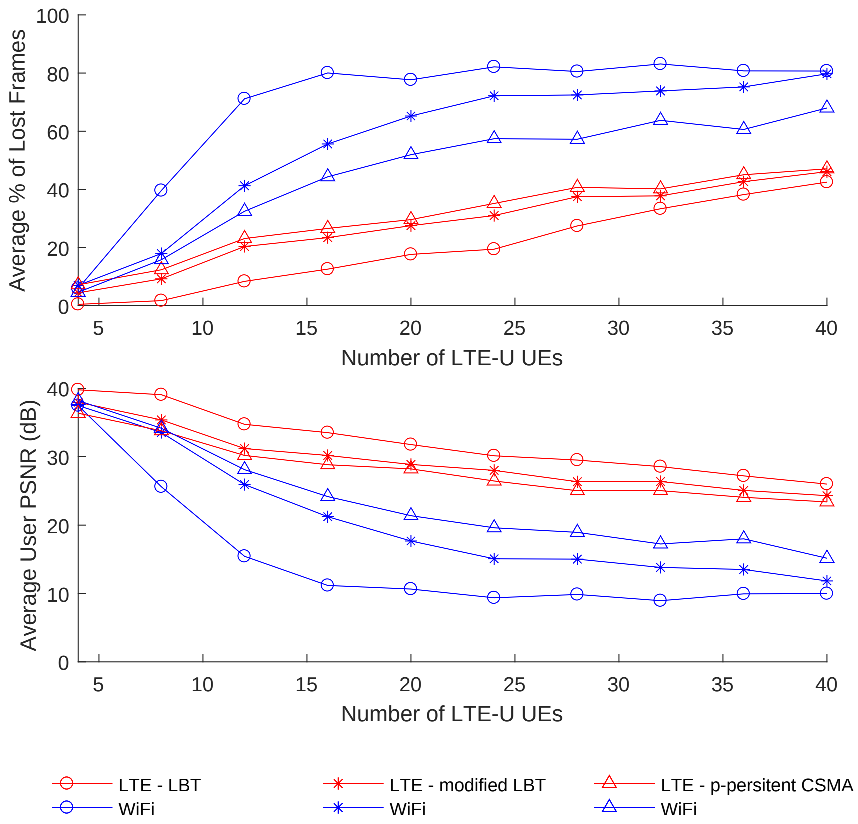

Figure 15: LTE-U/WiFi coexistence scenario using different LTE-U channel access mechanisms (a) percentage of lost frames (b) PSNR.

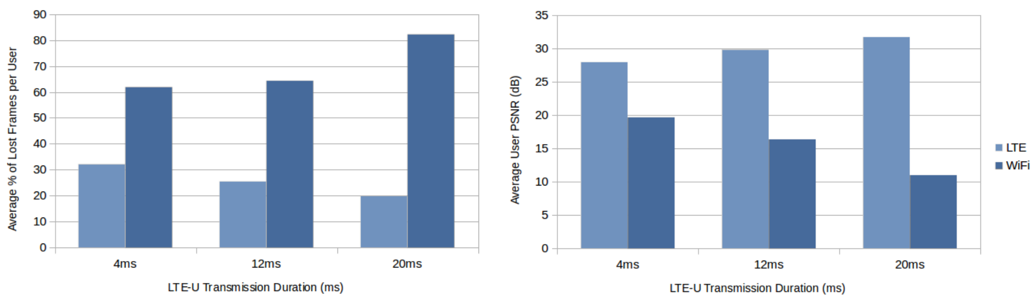

Figure 16: Effect of changing the $Txop$ parameter of the modified LBT scheme on the coexistence of LTE-U and WiFi.

as the competition in the unlicensed channel increases due to LTE transmitting a substantially larger number of frames over the unlicensed channel (29 P frames as opposed to 2 or 3 B frames). Moreover, the losses in LTE increase because a large portion of important information (all the p frames) are transmitted over the unlicensed spectrum.

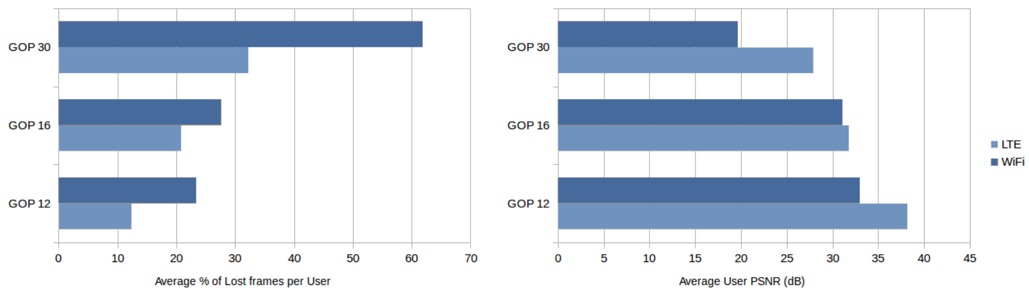

Figure 17: Effect of changing the GOP size on the LTE-U/WiFi coexistence using the modified LBT scheme.

For the adaptive p-persistent CSMA scheme, we run the simulations for five different values of I_{ED} and observe the effect on the quality of video received by the users. The results are illustrated in Figure 18. The results show that as the value of I_{ED} decreases, the losses for LTE increase while those for WiFi decrease. This is attributed to the fact that by lowering the energy detection threshold, LTE-U would constantly find the channel occupied and would defer transmission till the next time slot, which leaves more room for WiFi to transmit. Thus I_{ED} can be used as a design parameter to control the degree LTE-U channel access depends on WiFi transmissions and hence, achieve an acceptable trade-off with WiFi. Next, similar to the modified LBT case, the number of LTE and WiFi users were fixed to 20 users each and the energy detection threshold was fixed to -72 dBm. Different GOP sizes of the video were then tested to study the effect of changing the GOP structure on the quality of the video received by the users. The results are illustrated in Figure 18. The trend observed is similar to the modified LBT case. Hence, it can be concluded that using short GOP structures with intermediate B frames transmitted over the unlicensed channel achieves best results. The higher frequency of I frames in shorter GOP structures improves the quality of the decoded video. In addition, the smaller sizes of B frames (compared to I and P frames) means that they will cause less interference for WiFi when transmitted over the unlicensed channel.

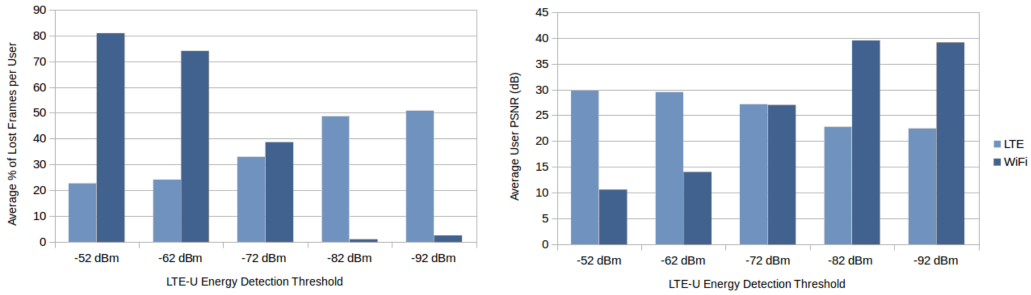

Figure 18: Effect of changing the energy detection threshold of the adaptive p-persistent CSMA scheme on the coexistence of LTE-U and WiFi.

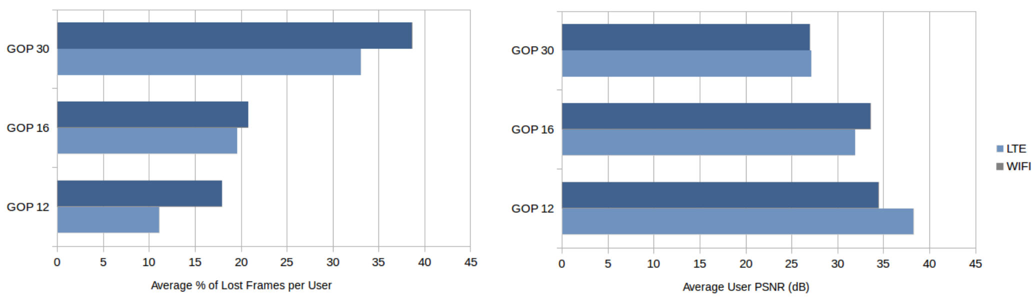

Figure 19: Effect of changing the GOP size on the LTE-U/WiFi coexistence using the adaptive p-persistent CSMA scheme.

Chapter 4: QoE-Based Dynamic Channel Selection

While the scheme proposed in Chapter 3 introduced a noticeable boost in the system performance for both LTE-U and WiFi, that scheme doesn't take into account the quality of the channel the frame is transmitted over. Certain situations may arise where, despite the presence of WiFi competition in the unlicensed spectrum, the quality of the unlicensed channel may still be superior to the quality of its licensed counterpart. Hence, transmitting a key frame over the licensed channel may increase the probability of its loss. Additionally, that scheme does not take advantage of the multiple channels available for use in the unlicensed spectrum which can be aggregated to improve the capacity of the LTE network and reduce interference to WiFi systems. In this chapter, an alternative approach to transmitting video over LTE-U is adopted where frames are dynamically assigned to a subset of channels depending on a certain number of factors that are UE-, frame-, and channel-specific.

4.1. Proposed Approach

The proposed scheme is based on a system model where the LTE eNB operates in a supplemental downlink mode. It has access to the licensed channel where it originally operates in addition to N unlicensed channels that are used to supplement the licensed channel if the need arises. Each frame of the video is assigned to one of the channels based on the solution to a multi-objective optimization problem that aims to maximize a certain set of utility functions. The main goal is to maintain QoE for the LTE UE while at the same time minimizing damage to WiFi.

QoE is a performance metric that reflects the general acceptability of the service as perceived subjectively by end-users [70]. When it comes to real-time communication services such as video transmission, focusing on the technical performance of the network reflected by QoS measures is not enough. Video streaming is an application in which the user perception plays a big role which the technical performance metrics do not necessarily reflect. Therefore, another metric is adapted here which is QoE that better reflects the user's experience and satisfaction. QoE can be measured using subjective or objective approaches. In this work we focus on objective approaches since they are more appropriate for our implementation [17].

Specifically, we have chosen to focus on two main aspects, namely the average PSNR of the received video and the frame delay. We provide a framework for predicting the expected average PSNR of a received video sequence over a flat fading channel based on the UE's SNR measurements in that channel. We also provide another framework for predicting the delay of a video frame over each channel based on the UE's past experiences using those channels. To minimize the interference caused to WiFi, the above two factors are coupled with another that indicates the probability of a channel being already occupied by a WiFi transmission. The three factors are combined into a multi-objective optimization problem, the solution of which assigns the different frames of the UEs to the different channels.

To model which channel a UE is assigned to, we define a binary variable, x_{ij} that indicates whether UE $i \in N_{UE}$ is assigned to channel $j \in N_{ch}$, viz.,

$$x_{ij} = \begin{cases} 1 & \text{if UE } i \text{ is assigned to channel } j \\ 0 & \text{Otherwise} \end{cases} \tag{5}$$

The rest of the notations are summarized in Table 4

4.1.1. SNR-based PSNR prediction framework

The factor that has the greatest effect on the user's viewing experience is the quality of the received frame. The most popular metric used to quantify that is the PSNR. Hence, the first objective function we formulate is one that aims to maximize the average PSNR of the received video sequence. Since the PSNR cannot be measured by the eNB before hand, it has to be predicted. Here, we outline a method for predicting the average PSNR of a received video sequence using the known SNR of the channel.

Recall from (3) that PSNR is defined as the ratio of the highest signal power to the corrupting noise power. Since the highest value a pixel can take is 255, the highest possible signal power is expressed as 255^2. The corrupting noise is quantified in (2) using the mean squared error (MSE) which is the average squared difference between the pixel values of the original frame and the pixel values of received corrupted frame.

Table 4: List of Notations

Symbol	Definition
x_{ij}	$x_{ij} = 1$ indicates UE i is assigned to channel j
N_{UE}	Number of LTE UEs
N_{ch}	Number of channels
PSNR_{ij}	expected PSNR of UE i over channel j
D_e	Distortion introduced by the encoder
D_v	Distortion introduced at the decoder
σ_{u0}^2	sensitivity of the decoder to an increase in error rate
σ_u^2	Energy of errors in a single frame
σ_v^2	Energy of propagated errors
γ	Efficiency of decoder's spatial loop filtering
β	Rate of Intra-coded frames
TBS_i	Transport Block size of UE i
BLER_{ij}	Block error rate of UE i over channel j
BER_{ij}	Bit error rate of UE i over channel j
SNR_{ij}	Signal to noise ration of UE i ocer channel j
BW_{ij}	Bandwidth allocated to UE i in channel j
$R_{b_{ij}}$	data rate of UE i in channel j
M	Number of modulation levels
T_s	Symbol duration
$N_{RB_{ij}}$	Number of resource blocks assigned to UE i in channel j
$\bar{\gamma}_{ij}$	Averaged received SNR of UE i over channel j
h	Channel gain
Th_{ij}	Expected throughput of UE i using channel j
r_{ij}	Throughput of UE i from the most recent usage of channel j
α	Learning rate
S_{ik}	Size of frame k of UE i
τ_{ik}	Deadline of frame k of UE i
p_j	Probability of LTE accessing unlicensed channel j
I_{ED}	Energy Detection Threshold
I_j	Interference power measured in channel j
I_{mean}	Average interference power in the unlicensed channel
σ_I	Variance of the interference power in the unlicensed channel
N_{RBG_j}	Number of Resource Block Groups available in channel j

Hence, to predict the PSNR, the MSE needs to be predicted first. The method adopted here is based on the one presented in [63] which links the MSE of a received video frame to the BER experienced over a channel. That analysis, however, is carried out for H.263 coded videos transmitted over binary symmetric channels using linear FEC schemes. It also does not take into account the effects of multipath fading on the BER of the received signal. Here, we extend that framework to MPEG4 coded videos transmitted over a lossy flat fading channel in LTE systems.

According to [63], the MSE averaged over all frames can be modeled as a summation of two types of distortions. The first is the distortion introduced by the encoder due to the loss of information caused by quantization. The second type of distortion is the distortion introduced by transmission errors which also propagate through several frames at the decoder due to the temporal dependencies between the frames. Hence the MSE can be expressed as follows.

$$\mathrm{MSE} = D_e + D_v, \tag{6}$$

where D_e is the distortion introduced by the encoder and D_v is the distortion introduced at the decoder. The distortion introduced by the encoder is codec specific and is independent of the state of the channel. Hence it can be treated as a constant in our analysis. The distortion introduced by the decoder, on the other hand, is dependent on the packet error rate which varies based on the state of the channel.

Pixel errors in each incorrectly decoded frame are considered as a corrupting signal that overlays the original frame and distorts the pixel values. The error signal is modeled as a zero-mean Gaussian random process $u(x,y)$ with variance σ_u^2. On average, the error signal is assumed to have the same variance in each frame. Due to the use of motion estimation and compensation that introduce temporal dependencies between the frames, errors introduced in one frame can propagate through several frames. Since, by definition, the MSE is the average difference between the original and erroneous frames, we can quantify the distortion at the decoder by accumulating the error signals of all the frames.

The variance of the error signal in a single frame σ_u^2 depends on many factors including implementation issues and the encoded video sequence. However, it is most directly linked to the information loss rate. An increased number of lost packets will increase the variance of introduced errors. Hence, the variance of the error σ_u^2 can be expressed as the multiplication of two factors, one representing the residual word error rate and the other representing the decoder's ability to cope with errors.

$$\sigma_u^2 = \sigma_{u0}^2 P_e, \tag{7}$$

where P_e is the residual word error rate and σ_{u0}^2 is a constant representing the sensitivity of the decoder to an increase in the error rate. The above is the variance of the error signal in a single frame. The variance of the propagated error is calculated in [63] by multiplying this with a power transfer factor that takes into account the effects of spatial loop filtering and the intra-coded frames. More specifically,

$$\sigma_v^2 = \sigma_u^2 \left(\frac{1 - \beta t}{1 + \gamma t} \right), \tag{8}$$

where γ is a leakage factor that represents the efficiency of spatial loop filtering at the decoder and β is the intra rate defined as $\frac{1}{T}$ where T is the GOP length. The maximum number of frames an error can propagate over is the number of frames in the GOP structure. That is because at the end of each GOP, a new I frame is inserted as the beginning of the new GOP. Hence the source of prediction is now the new I frame and the propagated error is reset to zero. Hence, the time averaged distortion introduced due to transmission errors can be obtained by combining the error signals in each frame in the GOP. Using the assumption that the error signals are uncorrelated from frame to frame, the distortion at the decoder can be calculated as

$$D_v = \sigma_u^2 \sum_{t=0}^{T-1} \frac{1 - \beta t}{1 + \gamma t}. \tag{9}$$

In LTE systems, the data handed from the MAC layer to the PHY layer are divided into units called Transport Blocks (TB). These are the units to which cyclic redundancy check (CRC) is applied to in order to detect transmission errors. Hence, we represent the residual error rate in our analysis as the block error rate (BLER). The linear relationship in (7), according to [63], is valid only for error rates less than 0.1 after which the frame quality is already is considerably deteriorated. Therefore, for our implementation purposes, this linear relationship is sufficient. The MSE is then expressed fully as

$$\text{MSE} = D_e + \sigma_{u0}^2 \text{BLER} \sum_{t=0}^{T-1} \frac{1-\beta t}{1+\gamma t}. \tag{10}$$

BLER depends on many factors including the state of the channel, the forward error correction scheme used, etc. LTE systems further divide the TBs into code blocks which then undergo channel coding. Due to the use of adaptive modulation and coding, the code rate varies among these blocks which makes it difficult to get a precise analytical expression for the probability of error in each block. Hence, we use an upper bound on the BLER that represents a worst case scenario. Assuming the bit errors in each LTE transport block are independent and identically distributed, the BLER can be estimated from the BER using the relation

$$\text{BLER}_{ij} = 1 - \left(1 - \text{BER}_{ij}\right)^{\text{TBS}_i}, \tag{11}$$

where TBS_i is the size of the transport block in bits of UE i. To predict the BLER of a UE over a channel beforehand, the BER of that UE over the channel is needed which is not available to the eNB. The eNB, however, does have access to the UE's SNR measurement, which is periodically reported by the UE to the eNB in each subframe. Next we link the BER achievable over a channel to the SNR measurements in that channel for LTE systems. For the sake of simplicity, we first carry out the analysis without taking multiplath fading into account, then we extend the results to account for fading effects.

Using the SNR value, the energy per bit to noise power spectral density $\frac{E_b}{N_0}$ is be found as

$$\frac{E_b}{N_0} = \text{SNR}\frac{BW}{R_b}, \tag{12}$$

where BW is the bandwidth allocated to the UE by the scheduler and R_b is the data rate. Since LTE employs OFDMA in the physical layer, the bandwidth is calculated through multiplying the number of resource blocks assigned to the UE by the bandwidth of one resource block. Hence, $BW_{ij} = N_{RB_{ij}} \times 180$ KHz where $N_{RB_{ij}}$ is the number of resource blocks assigned by the scheduler to UE i over channel j. The data rate R_b varies based on the bandwidth and the modulation and coding scheme used. Since subcarriers from multiple resource blocks are aggregated together in each LTE subframe, and each resource block comprises 12 subcarriers, the data rate of UE i over channel j is calculated as

$$R_{b_{ij}} = \log_2 M \times R_s \times 12 \times N_{RB_{ij}}, \tag{13}$$

where M is the number of possible symbols which varies based on the modulation scheme used and R_s is the OFDM symbol rate. $\frac{E_b}{N_0}$ is then used to calculate the expected BER depending on the modulation scheme used. Since LTE employs three types of modulation schemes, QPSK, 16QAM, and 64QAM all of which are square, the BER can be generally expressed as follows.

$$\text{BER} = 1 - \left(1 - 2\left(1 - \frac{1}{\sqrt{M}}\right) Q\left(\sqrt{\frac{3\log_2 M}{M-1}\frac{E_b}{N_0}}\right)\right)^2. \tag{14}$$

Using (12) and substituting back in (11) we get an expression for predicting the BLER using the UE's measured SNR value.

$$\text{BLER}_{ij} = 1 - \left(\left(1 - 2\left(1 - \frac{1}{\sqrt{M}}\right) Q\left(\sqrt{\frac{3\log_2 M}{M-1}\text{SNR}_{ij}\frac{BW_{ij}}{R_{b_{ij}}}}\right)\right)^2\right)^{\text{TBS}_i}. \tag{15}$$

Hence, the MSE can be predicted as

$$\text{MSE}_{ij} = D_e + \sigma_{u0}^2\left(1 - \left(\left(1 - 2\left(1 - \frac{1}{\sqrt{M}}\right) Q\left(\sqrt{\frac{3\log_2 M}{M-1}\text{SNR}_{ij}\frac{BW_{ij}}{R_{b_{ij}}}}\right)\right)^2\right)^{\text{TBS}_i}\right)\sum_{t=0}^{T-1}\frac{1-\beta t}{1+\gamma t}. \tag{16}$$

The result in (16) is applicable for lossy channels without taking the effects of fading into account. This somewhat diminishes its accuracy since fading greatly affects the probability of erroneous reception of a block. Due to multipath propagation, multiple copies of the signal arrive at the receiver being reflected, diffracted, and/or scattered off different objects. The signal detected at the receiver is a superposition of several delayed and phase shifted copies of the signal which add constructively or destructively, hence distorting the amplitude of the original signal. Therefore, we next extend the analysis above to take into account the effects of a fading channel. We consider a flat fading channel where the different frequency components of the signal all experience the same level of attenuation. The magnitude of the signal attenuation h is assumed to be a Rayleigh distributed random variable. The average received SNR, $\bar{\gamma}$ is defined as

$$\bar{\gamma} = \frac{E_b}{N_0} E\left[h^2\right] = \mathrm{SNR}\frac{BW}{R_b} E\left[h^2\right], \tag{17}$$

where $E\left[h^2\right]$ is the mean instantaneous power of the fading channel. The BER of M-QAM modulation scheme in AWGN and Rayleigh fading channel is give in [71] as

$$\mathrm{BER} = \frac{2}{\log_2 M}\left(1 - \frac{1}{\sqrt{M}}\right)\sum_{i=1}^{\frac{\sqrt{M}}{2}} 1 - \sqrt{\frac{1.5\,(2i-1)^2\,\bar{\gamma}\log_2 M}{M - 1 + 1.5\,(2i-1)^2\,\bar{\gamma}\log_2 M}}. \tag{18}$$

Substituting back into 11, we get an expression for the BLER of a UE's M-QAM modulated signal in a Rayleigh fading channel,

$$\mathrm{BLER}_{ij} = 1 - \left(1 - \left(\frac{2}{\log_2 M}\left(1 - \frac{1}{\sqrt{M}}\right)\sum_{i=1}^{\frac{\sqrt{M}}{2}} 1 - \sqrt{\frac{1.5\,(2i-1)^2\,\bar{\gamma}_{ij}\log_2 M}{M - 1 + 1.5\,(2i-1)^2\,\bar{\gamma}_{ij}\log_2 M}}\right)\right)^{\mathrm{TBS}_i}. \tag{19}$$

The MSE is then predicted as

$$\mathrm{MSE}_{ij} = D_e + \sigma_{u0}\left(1 - \left(1 - \left(\frac{2}{\log_2 M} \times \left(1 - \frac{1}{\sqrt{M}}\right)\sum_{l=1}^{\frac{\sqrt{M}}{2}} 1 - \sqrt{\frac{1.5\,(2l-1)^2\,\bar{\gamma}_{ij}\log_2 M}{M - 1 + 1.5\,(2l-1)^2\,\bar{\gamma}_{ij}\log_2 M}}\right)\right)^{\mathrm{TBS}_i}\right)\sum_{t=0}^{T-1}\frac{1-\beta t}{1+\gamma t}. \tag{20}$$

Hence, the only thing that the eNB needs to estimate the PSNR achieved by transmitting the frame over a certain channel is the UE's SNR measurement in that channel. The other parameters σ_{u0}^2, γ, and D_e are constants that are provided by the server for each video sequence.

The first objective function is then expressed as

$$\max \frac{1}{N_{ch}} \frac{1}{N_{UE}} \sum_{j=1}^{N_{ch}} \sum_{i=1}^{N_{UE}} x_{ij} \mathrm{PSNR}_{ij}, \tag{21}$$

where N_{ch} is the total number of channels, N_{UE} is the total number of UEs and $PSNR_{ij}$ is the average expected PSNR of UE i's video over channel j.

4.1.2. Frame delay prediction

In order to maintain continuous video playback at the receiver, each frame must arrive before its deadline. In other words, for continuous playback to be maintained, the time that it would take the frame to arrive at the receiver must be less than the time leading up to the frame deadline. We estimate that time by dividing the frame size by the expected throughput achievable over the channel, in other words

$$\text{Frame delivery time} = \frac{\text{Frame size}}{\text{Throughput}}. \tag{22}$$

The expected throughput over a channel is calculated for each UE in a moving average fashion similar to [33] where the achievable throughput for a UE over a channel is a combination of the UE's past experience using the channel and the throughput in the most recent usage of the channel. Equation 23 further illustrates this.

$$Th_{ij} = (1-\alpha) Th_{ij} + \alpha r_{ij}, \tag{23}$$

where Th_{ij} is the expected throughput of UE i using channel j, r_{ij} is the throughput achieved after the last usage of the channel, and α is the learning rate which is a design parameter that determines how much does the calculated value depend on the current usage of the channel versus the past experience. After each packet reception, the UE evaluates (23) and informs the eNB with the value.

Hence, the second objective function can be formed by taking the difference between the frame delivery time defined in (22) and the frame deadline period. Subtracting these two intervals will show us the duration of time the frame falls short of meeting it's deadline. The goal here is minimize this period so as to guarantee as many timely arrivals of frames as possible.

$$\min \frac{1}{N_{ch}} \frac{1}{N_{UE}} \sum_{j=1}^{N_{ch}} \sum_{i=1}^{N_{UE}} x_{ij} \left(\frac{S_{ik}}{Th_{ij}} - \tau_{ik} \right), \tag{24}$$

where S_{ik} is the size in bits of frame k of UE i, Th_{ij} is the expected throughput of UE i over channel j, and τ_{ik} is the deadline of frame k of UE i.

4.1.3. Coexistence with WiFi

While it is very important to guarantee the quality and timely delivery of the LTE UE frames, it is also equally important to limit the interference caused to WiFi. This can be achieved by trying to select the channel that is least likely to be occupied by a WiFi transmission. Adopting the p-Persistent CSMA channel access scheme proposed in [24], the probability of WiFi transmissions being present in the channel can be calculated using the probability of LTE accessing the channel p. This is modeled using a complementary Gaussian distribution function of the energy detection results performed by the eNB. As mentioned in Chapter 3, the mean of the distribution is equal to the energy detection threshold. The standard deviation of the distribution is a design parameter that can be used to control the shape of the distribution. A narrow distribution where the mean equals the energy detection threshold is preferred to ensure that the probability of LTE accessing the channel is high when the sensed interference is below the energy detection threshold and low when the sensed interference is above the energy detection threshold.

The probability of WiFi transmissions being present in the channel can then be calculated by taking the complement of p. Hence, striving to reduce the interference caused to WiFi, the eNB should select the channel with the least probability of WiFi presence. This is an extension of dynamic channel selection proposed in the literature where, instead of detecting whether a channel is busy or not and putting a hard limit on it (a yes or no situation), we assign to each channel a probability of how likely the channel is to be occupied by a WiFi device, and hence allow for more accuracy in selecting the channel.

The third objective function is then formed as

$$\min \frac{1}{N_{ch}} \frac{1}{N_{UE}} \sum_{j=1}^{N_{ch}} \sum_{i=1}^{N_{UE}} x_{ij} \left(1 - P_j\right), \tag{25}$$

where $\left(1 - P_j\right)$ is the probability of channel j being occupied by a WiFi device.

4.1.4. Channel selection optimization problem

So far, three factors are involved in making the decision of which channel to transmit a UE's frame over. These factors are the average UE PSNR, the average UE delay, and the probability of WiFi being present in the channel defined by the objectives (21), (24), and (25) respectively. These objectives are of conflicting nature. A channel that may provide the best PSNR for a UE may also be the channel that is most populated by WiFi. In addition, while a channel with better quality improves the throughput hence decreasing the delay, a channel with a larger number of WiFi users reduces the throughput hence increasing the delay. Due to the conflicting nature of these objectives, multi-objective optimization is employed to solve the frame assignment problem.

Since no single solution exists that can simultaneously optimize all objectives, some sort of trade-off must be managed. This trade-off is achieved by assigning a different priority for each objective. Three priority levels are defined in our formulation for the above factors. Since WiFi performance is somewhat protected by employing the time-sharing channel access scheme discussed in Section 4.1.3, the WiFi protection factor is given the lowest priority in the optimization formulation. The other two LTE-related factors are given higher priorities, with PSNR being the highest followed by frame delay. The logic followed here is that, while the continuity of playback is an important factor of the UE's QoE, if the quality of the received video is low, the user's viewing experience is greatly affected.

In terms of constraints, each UE must be assigned to one channel only in the duration of a single frame transmission, hence the first constraint is expressed as:

$$\sum_{i} x_{ij} = 1. \tag{26}$$

The LTE standard groups the resource blocks in each channel into resource block groups (RBG). The number of resource blocks per RBG depends on the type of the resource allocation employed by the MAC layer. Each UE is assigned to one RBG by the scheduler. Hence, to ensure that the amount of resources assigned to UEs does not exceed the amount of resources available in each channel, we formulate the second constraint to limit the number of UEs assigned to each channel to the number of RBGs available in that channel, viz.,

$$\sum_{j} x_{ij} \leq N_{RBG_j}. \tag{27}$$

The final problem is formulated as

$$\begin{gathered}
\max \frac{1}{N_{ch}} \frac{1}{N_{UE}} \sum_{j=1}^{N_{ch}} \sum_{i=1}^{N_{UE}} x_{ij} PSNR_{ij}, \\
\min \frac{1}{N_{ch}} \frac{1}{N_{UE}} \sum_{j=1}^{N_{ch}} \sum_{i=1}^{N_{UE}} x_{ij} \left(\frac{S_{ik}}{Th_{ij}} - \tau_{ik} \right), \\
\min \frac{1}{N_{ch}} \frac{1}{N_{UE}} \sum_{j=1}^{N_{ch}} \sum_{i=1}^{N_{UE}} x_{ij} \left(1 - p_j\right), \\
s.t. \\
\sum_{i} x_{ij} = 1, \\
\sum_{j} x_{ij} \leq N_{RBG_j}, \\
x_{ij} \in \{0, 1\}.
\end{gathered} \tag{28}$$

The first objective function aims to maximize the average user PSNR over the different channels. The second objective function aims to minimize the delay in the reception of frames by minimizing the average time the frame falls short of meeting its deadline. The third objective function aims to minimize the annoyance caused to

WiFi by minimizing the average probability of selecting a channel already occupied by a WiFi device. Users are allocated to each channel based on the solution to this optimization problem which is carried out on a frame basis.

To solve the above problem, the lexicographic approach is adopted where the objective functions are optimized one at a time in a decreasing priority order [72]. After each step, the solution to the previous objective function is added as an equality constraint to the next objective function. In other words, when optimizing for one objective, only the solutions that wouldn't degrade the higher-priority objectives are considered. Some solvers such as the one adopted in this work allow this constraint to be relaxed a bit by specifying a tolerance value for each objective. This indicates the fraction of the optimal value of this objective that the lower priority objectives are allowed to degrade it by.

Implementation wise, the HeNB sends a reference signal to the UE over each of the channels. Based on the received signal, the UE calculates the SNR for each channel and sends it to the HeNB along with the average past throughput over each channel, the CQI of each channel, and the buffer status report (BSR). This process is repeated in every subframe. For each video frame of each UE, based on the CQI and BSR information received from the UE, the scheduler in the HeNB decides the best allocation of resources to the UE over each channel. Then, using that along with the SNR, throughput, and video frame information, the HeNB calculates the expected PSNR and delay of the frame over each channel. The HeNB also calculates the probability of WiFi presence in each channel based on energy detection results. Using this information, the HeNB decides the best channel to transmit the frame over based on the solution to 4.1.4.

4.2. Performance Evaluation

The above proposed approach is simulated using the integration of three softwares, namely NS-3, evalvid, and Gurobi optimizer as shown in Figure 20. Evalvid is a video quality evaluation software that is responsible for encoding the raw video into a compressed MP4 format, hinting the MP4 track, and generating a trace file that includes information about the video sequence. This information includes frame types,

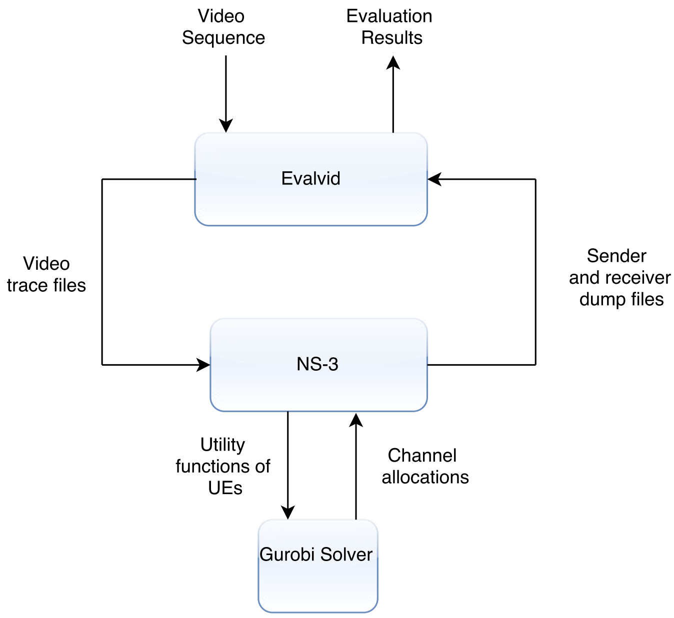

Figure 20: Simulation setup.

frame sizes, number of packets in each frame, and frame send times. The trace files are then fed into NS-3 which is responsible for simulating the wireless network architecture and the actual video transmission. It simulates the scenario consisting of the LTE network including the epc, eNBs and UEs, the WiFi network including the APs and STAs, the wireless channels, and the server-client interaction. An Evalvid module is integrated within NS-3 that reads the content of the trace files, generates video packets accordingly, and transmits them through the designated sockets. An optimization software called Gurobi is also integrated within NS-3 as external library that is called to solve the optimization problem formulated in Section 4.1. The simulation output consists of server and client dump files generated by NS-3 which are then fed to Evalvid to decode the video received by each user. Using the decoded video file, it then calculates the percentage of lost frames, end-to-end delay, and PSNR among other parameters.

4.2.1. Simulation scenario

Similar to Chapter 3, we consider the scenario where an LTE and a WiFi small cell coexist in the same geographical area with a separation of d m. The LTE cell consists of a home e-Node B (HeNB) operating in the licensed channel to which it originally has access in addition to m unlicensed channels, serving N user equipment (UEs). The WiFi cell consists of a WiFi access point (AP) and N WiFi stations (STAs).

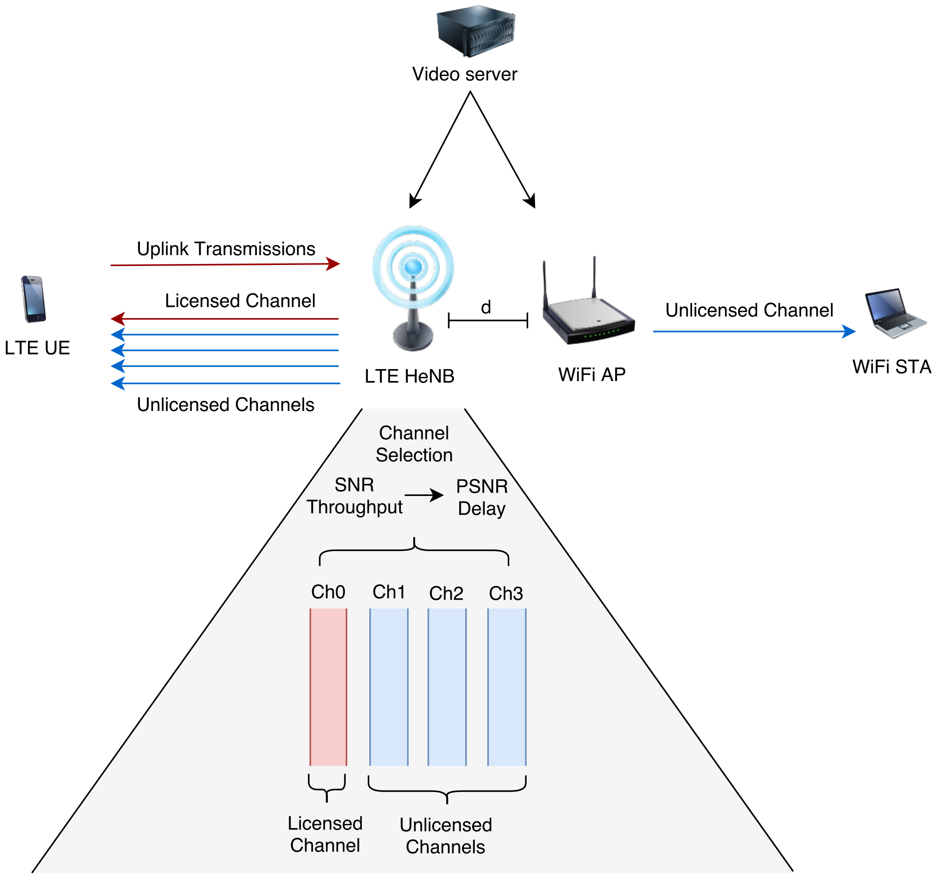

Figure 21: System model for the QoE-based dynamic channel selection scheme.

The same number of WiFi APs and STAs occupy each of the unlicensed channels. The N users of each cell are moving randomly within the area. Control and signaling information as well as uplink data of LTE are communicated over the licensed spectrum while the downlink data is split over the licensed and m unlicensed channels according to the scheme discussed in Section 4.1 and illustrated in Figure 21. A remote server is sending a video sequence to each of the UEs and STAs through the LTE HeNBs and the WiFi APs. All video files are compressed before transmission to reduce the file size. The scheduler used in the simulation is a proportional fair one. The propagation model used is the Rayleigh propagation model. The number of unlicensed channels used is 4. The remaining simulation parameters are summarized in Table 5. The video file used is the "Foreman" test sequence and is encoded using an MPEG-4 codec at a bit rate of 2 Mbps. The resolution of the sequence is 352×288 and it consists of 300 frames with a total duration of 10 seconds.

Table 5: Simulation Parameters for the QoE-based dynamic channel selection scheme.

Parameter	Value
WiFi Standard	802.11n
Number of LTE cells	4
Number of WiFi cells per channel	4
Channel BW	20 MHz (100 RBs)
Number of unlicensed channels	4
Center frequencies of unlicensed channel	5.18, 5.20, 5.22, 5.24 GHz
Center frequency of licensed channel	2.12 GHz
LTE scheduler	Proportional fair
LTE Resource Allocation Type	Type 0 (4 RBs per RBG)
LTE channel access duration	4ms
LTE Backoff duration	1ms
Energy Detection Threshold	-72 dBm
Standard deviation of P_j	9 dBm
Channel model	Rayleigh propagation model
Separation of WiFi AP and LTE HeNB	5m
Distribution of users location	Uniform random distribution
Speed of UEs	3 km/h
Antenna Type	Isotropic
HeNB/AP power	18 dBm
UE/STA power	18 dBm
UE noise figure	9 dB

4.2.2. Simulation results

To evaluate the effectiveness of our proposed scheme, another scenario is proposed and simulated. The second scheme also employs p-persistent CSMA as a channel access mechanism in the unlicensed channels, but the frames are assigned to channels in a random fashion. The results are shown in Figure 22. Four performance metrics are used to evaluate the effectiveness of our proposed scheme, namely the average percentage of lost frames per user, the average user PSNR, the average user end-to-end delay, and the average cumulative jitter. The results show that, for both schemes, as the number of LTE-U UEs increases, the number of lost frames, delay, and jitter for both LTE-U

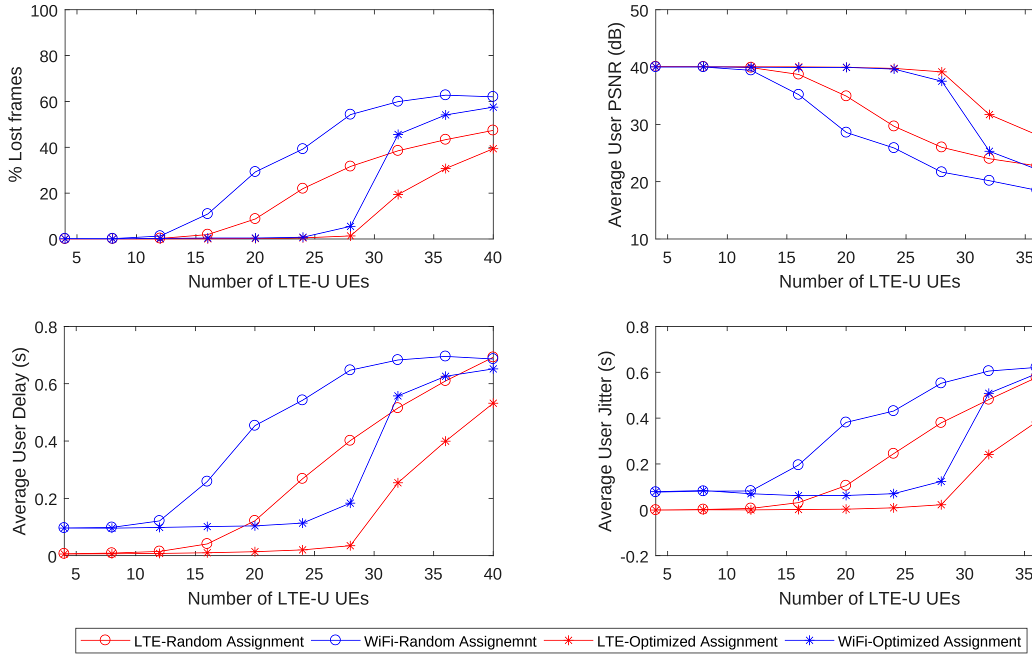

Figure 22: QoE-based frame assignment scheme compared to random assignment (a) Percentage of lost frames (b) Average user PSNR (c) Average user delay (d) Average user Jitter.

and WiFi users increase while the average PSNR of the received video decreases. This degradation in performance is expected as UEs get assigned less resources and WiFi users experience more competition in the unlicensed spectrum.

For small numbers of UEs, both the optimized and random schemes perform similarly as the resources available in the channels are enough to accommodate all users. As the number of UEs increases, we find that the optimized frame assignment scheme significantly outperforms the random assignment scheme in terms of reducing the percentage of lost frames, delay, and jitter, and improving the average PSNR. More specifically, the average PSNR of the received video improved by a maximum of 15.87 dB for WiFi and 13.16 dB for LTE-U. The delay of the received video decreased by a maximum of 0.46 seconds for WiFi and 0.37 seconds for LTE-U. The frame loss rate was reduced by a maximum of 48.75% for WiFi and 30.3% for LTE-U. This performance improvement is attributed to the fact that UEs are assigned to the channels over which they are expected to achieve the maximum PSNR and minimum delay, hence, the overall quality of the UE videos increases. In addition, the UEs are assigned to the channels with the least probability of being occupied by a WiFi transmission, hence the likelihood of collisions is significantly reduced and a better performance for both systems is experienced.

Compared to the other performance metrics, the greatest improvement is noticed for the PSNR, as that had the highest priority in our problem formulation. Following the argument proposed at the beginning of the chapter, channels vary in their quality regardless of the number of WiFi devices occupying them. A channel can have a small number of WiFi devices transmitting in it while at the same time exhibiting bad quality. Hence, we prioritize quality over competition and instead of always choosing the cleanest channel, we give higher priority to the channels with better condition. However, coexistence with WiFi is still an important issue as we are trying to protect WiFi transmissions as much as we can and reduce collisions. Hence, in the third objective function, we try to select the channels with the least likelihood of ongoing WiFi transmissions.

The simulation results also confirm that time-sharing coexistence schemes are not as effective on their own. The random assignment scheme simulated above also employs p-Persistent CSMA, an access scheme that shares the channel in time with WiFi. However, that alone is not enough to guarantee a good performance for both technologies. Similarly, simply extending LTE-U operation to multiple unlicensed channels without a specific channel selection criteria is not effective on its own either, even with the use of an effective time-sharing coexistence mechanism. The best performance is achieved by coupling adaptive channel selection schemes with time-sharing channel access mechanisms.

To quantify the damage caused to WiFi by LTE-U accessing the unlicensed spectrum using our proposed scheme, we simulate another scenario where two WiFi operators coexist in the same unlicensed channel. We simulate the same scenario above where 4 cells occupy the same building and sweep the number of WiFi users in each cell from 1 to 10. We then observe the average user frame loss and PSNR for each operator. The simulation results are illustrated in Figure 23. Comparing the LTE-U/WiFi scenario to the WiFi/WiFi scenario, we notice that the performance degradation caused to WiFi users by sharing the channel with an LTE-U small cell is less than that caused by sharing the channel with another WiFi cell. Since LTE-U smartly strives to select the channel with the least probability of an ongoing WiFi transmission in it, the collisions between the two technologies is significantly decreased and WiFi users experience a better performance.

Additionally, to quantify the gain obtained by LTE-U accessing the unlicensed channel using our proposed scheme, we simulate another scenario where the whole video is transmitted over the licensed channel only. The simulation results are illustrated in Figure 24. Comparing the two scenarios, we find that there is a considerable perfromance improvement to be gained by extending LTE's operation to the unlicensed channel using our scheme. For the largest number of LTE-U UEs, the performance improvement gained using our proposed scheme is 31.55% reduction in percentage of lost frames and 6.43 dB improvement in the average UE PSNR. By aggregating multiple unlicensed channels, the overall bandwidth available for LTE-U is significantly increased, allowing it to accommodate more users who are all requesting bandwidth-hungry applications at the same time. In addition to the increased aggregate bandwidth, LTE-U has more options, in terms of the channels available for it to transmit over. The licensed channel may not always exhibit the best quality. By calculating the expected PSNR and delay achieved by transmitting the video over each channel, LTE-U can choose the best channel to transmit a video frame over that will guarantee it the best results.

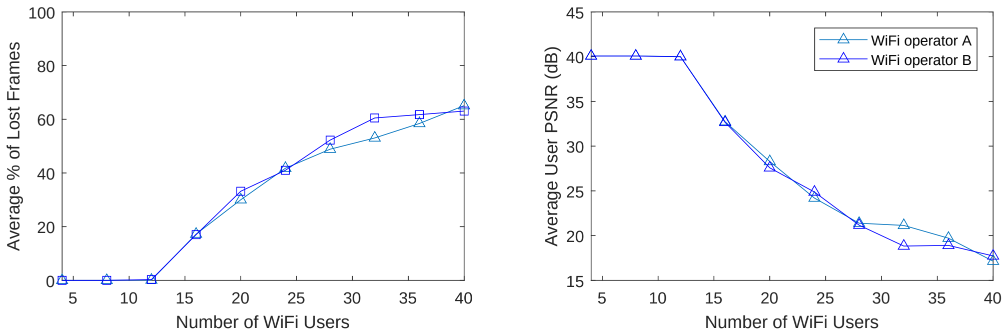

Figure 23: Two WiFi operators coexisting in the same channel (a) Percentage of lost frames (b) Average user PSNR.

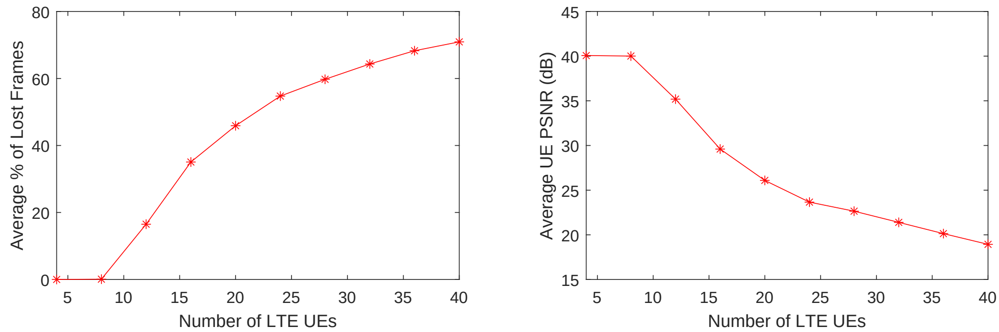

Figure 24: LTE's performance when the entire video is transmitted over the licensed channel (a) Percentage of lost frames (b) Average user PSNR.

Chapter 5: Conclusion

In this thesis, we have presented two channel selection schemes for video transmission over LTE-U. The first is a static channel selection scheme that divides the video frames over channels based on the sensitivity of the information in each frame type. We have coupled that scheme with different channel access mechanisms and compared their performance through extensive simulations. We have also studied the effect of varying the key design parameter of each channel access mechanism and the effect of changing the GOP structure of the encoded video file on the overall performance of the system.

Our findings confirm that for sensing-based channel access mechanisms, the energy detection threshold plays a key role in controlling the amount of interference caused to WiFi. By raising the energy detection threshold, a higher protection level can be achieved for WiFi at the expense of lower performance for LTE-U. In terms of the encoded video's GOP structure, shorter GOP structures provide better performance since the higher frequency of reference frames in those structures limits the error propagation.

The second proposed scheme is a dynamic channel selection scheme that assigns user frames to different channels based on the solution to a multi-objective optimization problem that takes into account the predicted quality of the received video in each channel, the expected average frame delay, and the probability of causing interference to WiFi transmissions. We have presented a framework for predicting the average PSNR of a received video over a flat fading channel using the SNR measurements in that channel. We have also presented a framework for predicting the average frame delay over a channel based on the UE's past experiences using the channel. Through extensive simulations we have evaluated the performance of this channel selection scheme and compared it to another scheme that employs the same-time sharing channel access mechanism but assigns frames to channels randomly. The simulation results show that our dynamic channel scheme achieves a significantly better performance in terms of improving the received video quality and reducing the inter-frames delay for both LTE-U and WiFi users.

Our findings confirm that time-sharing coexistence mechanisms are not effective on their own and the need arises to extend the LTE-U transmission to multiple channels. However, aggregating multiple unlicensed channels does not always delivers the best performance unless a proper channel selection scheme is employed. Otherwise, selecting channels randomly will result in a performance degradation for both LTE-U and WiFi users. We also find that the quality of a channel is not necessarily always related to the amount of WiFi interference experienced in that channel. Even if the number of WiFi transmissions in a channel is small, that channel may still experience a worse quality due to a number of other factors. In our design, we have taken that into account by extending our selection criteria to include the SNR and throughput of the UEs over each channel in addition to the probability of ongoing WiFi transmissions in those channel.

Future research directions we propose include integrating the current framework with Dynamic Adaptive Streaming over HTTP (DASH) and scalable video coding, and deriving SNR-BER analytical expressions for other channel models.

References

[1] Cisco, "Cisco visual networking index: Global mobile data traffic forecast update, 2016-2021," white paper, Feb 2017.

[2] S. Pociask. (2015) We're three year away from spectrum shortages. Internet. [Online]. Available: https://www.forbes.com/sites/realspin/2015/06/30/the-spectrum-shortage-is-coming/#64d6a5eb55e9 [Accessed: 2017].

[3] OPENWAVE, "Media optimization for mobile networks: An intelligent solution to reduce costs, enhance the user experience and improve network efficiency," white paper, June 2010.

[4] A. Aijaz, H. Aghvami, and M. Amani, "A survey on mobile data offloading: technical and business perspectives," *IEEE Wireless Communications*, vol. 20, no. 2, pp. 104–112, April 2013.

[5] Q. Chen *et al.*, "Cellular meets WiFi: Traffic offloading or resource sharing?" *IEEE Transactions on Wireless Communications*, vol. 15, no. 5, pp. 3354–3367, May 2016.

[6] J. Wannstrom. (2013) LTE-Advanced. Internet. [Online]. Available: http://www.3gpp.org/technologies/keywords-acronyms/97-lte-advanced [Accessed: 2017].

[7] FCC. Accessing spectrum. Internet. [Online]. Available: https://www.fcc.gov/general/accessing-spectrum [Accessed: 2017].

[8] M. Condoluci *et al.*, "LTE-direct vs. WiFi-direct for machine-type communications over LTE-A systems," in *2015 IEEE 26th Annual International Symposium on Personal, Indoor, and Mobile Radio Communications (PIMRC)*, Aug 2015, pp. 2298–2302.

[9] R. Zhang *et al.*, "LTE-unlicensed: the future of spectrum aggregation for cellular networks," *IEEE Wireless Communications*, vol. 22, no. 3, pp. 150–159, June 2015.

[10] A. M. Voicu, L. Simi, and M. Petrova, "Coexistence of pico- and femto-cellular LTE-unlicensed with legacy indoor Wi-Fi deployments," in *2015 IEEE International Conference on Communication Workshop (ICCW)*, June 2015, pp. 2294–2300.

[11] J. Jeon *et al.*, "LTE with listen-before-talk in unlicensed spectrum," in *2015 IEEE International Conference on Communication Workshop (ICCW)*, June 2015, pp. 2320–2324.

[12] 3GPP. LTE. Internet. [Online]. Available: http://www.3gpp.org/technologies/keywords-acronyms/98-lte [Accessed: 2017].

[13] (2016, May) LTE tutorial. Internet. [Online]. Available: http://www.tutorialspoint.com/lte/ [Accessed: 2016].

[14] F. Firmin. The evolved packet core. Internet. [Online]. Available: http://www.3gpp.org/technologies/keywords-acronyms/100-the-evolved-packet-core [Accessed: 2017].

[15] Cisco, "Wireless LAN switches' functions and deployment," *The Internet Protocol Journal*, vol. 9, no. 3, 2016.

[16] M. Ghanbari, *Standard Codecs: Image compression and advanced video coding*. Institution of Engineering and Technology, 2011.

[17] K. Piamrat *et al.*, "Quality of Experience measurements for video streaming over wireless networks," in *2009 Sixth International Conference on Information Technology: New Generations*, April 2009, pp. 1184–1189.

[18] 3GPP, "Review of regulatory requirements for unlicensed spectrum," AlcatelLucent, Alcatel-Lucent Shanghai Bell, Ericsson, Huawei, HiSilicon, IAESI, LG, Nokia, NSN, Qualcomm, NTT Docom, Tech. Rep. RP-140808, June 2014.

[19] J. Xiao and J. Zheng, "An adaptive channel access mechanism for LTE-U and WiFi coexistence in an unlicensed spectrum," in *2016 IEEE International Conference on Communications (ICC)*, May 2016, pp. 1–6.

[20] A. Bhorkar *et al.*, "Medium access design for LTE in unlicensed band," in *2015 IEEE Wireless Communications and Networking Conference Workshops (WCNCW)*, March 2015, pp. 369–373.

[21] R. Yin *et al.*, "LBT-based adaptive channel access for LTE-U systems," *IEEE Transactions on Wireless Communications*, vol. 15, no. 10, pp. 6585–6597, Oct 2016.

[22] Q. Zhang *et al.*, "Design and performance analysis of a fairness-based License-Assisted Access and resource scheduling scheme," *IEEE Journal on Selected Areas in Communications*, vol. 34, no. 11, pp. 2968–2980, Nov 2016.

[23] B. Jia and M. Tao, "A channel sensing based design for LTE in unlicensed bands," in *2015 IEEE International Conference on Communication Workshop (ICCW)*, June 2015, pp. 2332–2337.

[24] B. Jia, "An adaptive p-persistent CSMA scheme for LTE in unlicensed bands," in *2015 International Conference on Wireless Communications Signal Processing (WCSP)*, Oct 2015, pp. 1–5.

[25] V. Valls *et al.*, "Maximizing LTE capacity in unlicensed bands (LTE-U/LAA) while fairly coexisting with 802.11 WLANs," *IEEE Communications Letters*, vol. 20, no. 6, pp. 1219–1222, June 2016.

[26] R. Zhang *et al.*, "Modeling and analysis of MAC protocol for LTE-U co-existing with Wi-Fi," in *2015 IEEE Global Communications Conference (GLOBECOM)*, Dec 2015, pp. 1–6.

[27] H. Ko, J. Lee, and S. Pack, “A fair listen-before-talk algorithm for coexistence of LTE-U and WLAN,” *IEEE Transactions on Vehicular Technology*, vol. 65, no. 12, pp. 10 116–10 120, Dec 2016.

[28] R. Al-Khansa and H. Artail, “A semi-distributed LTE-WiFi system design for future LTE-unlicensed: Deployments in small-cell environments,” in *2015 IEEE 11th International Conference on Wireless and Mobile Computing, Networking and Communications (WiMob)*, Oct 2015, pp. 43–50.

[29] Qualcomm, “Qualcomm research LTE in unlicensed spectrum: Harmonious coexistence with Wi-Fi,” Qualcomm Technologies, Inc., Tech. Rep., June 2014.

[30] T. Nihtil *et al.*, “System performance of LTE and IEEE 802.11 coexisting on a shared frequency band,” in *2013 IEEE Wireless Communications and Networking Conference (WCNC)*, April 2013, pp. 1038–1043.

[31] E. Almeida *et al.*, “Enabling LTE/WiFi coexistence by LTE blank subframe allocation,” in *2013 IEEE International Conference on Communications (ICC)*, June 2013, pp. 5083–5088.

[32] C. Cano and D. J. Leith, “Coexistence of wifi and LTE in unlicensed bands: A proportional fair allocation scheme,” in *2015 IEEE International Conference on Communication Workshop (ICCW)*, June 2015, pp. 2288–2293.

[33] O. Sallent *et al.*, “Learning-based coexistence for LTE operation in unlicensed bands,” in *2015 IEEE International Conference on Communication Workshop (ICCW)*, June 2015, pp. 2307–2313.

[34] A. M. Baswade *et al.*, “Unlicensed carrier selection and user offloading in dense LTE-U networks,” in *2016 IEEE Globecom Workshops (GC Wkshps)*, Dec 2016, pp. 1–6.

[35] F. S. Chaves *et al.*, “LTE UL power control for the improvement of LTE/Wi-Fi coexistence,” in *2013 IEEE 78th Vehicular Technology Conference (VTC Fall)*, Sept 2013, pp. 1–6.

[36] F. M. Abinader *et al.*, “Enabling the coexistence of LTE and Wi-Fi in unlicensed bands,” *IEEE Communications Magazine*, vol. 52, no. 11, pp. 54–61, Nov 2014.

[37] H. Song and X. Fang, “A spectrum etiquette protocol and interference coordination for LTE in unlicensed bands (LTE-U),” in *2015 IEEE International Conference on Communication Workshop (ICCW)*, June 2015, pp. 2338–2343.

[38] F. Cai *et al.*, “Spectrum sharing for LTE and WiFi coexistence using decision tree and game theory,” in *2016 IEEE Wireless Communications and Networking Conference*, April 2016, pp. 1–6.

[39] M. Zhang *et al.*, “Dynamic uplink radio access selection of LTE Licensed-Assisted Access to unlicensed spectrum: An optimization game,” *IEEE Communications Letters*, vol. 20, no. 12, pp. 2510–2513, Dec 2016.

[40] X. Yuan *et al.*, "Coexistence between Wi-Fi and LTE on unlicensed spectrum: A human-centric approach," *IEEE Journal on Selected Areas in Communications*, vol. 35, no. 4, pp. 964–977, April 2017.

[41] Q. Chen *et al.*, "Embedding LTE-U within Wi-Fi bands for spectrum efficiency improvement," *IEEE Network*, vol. 31, no. 2, pp. 72–79, March 2017.

[42] F. Liu *et al.*, "Small-cell traffic balancing over licensed and unlicensed bands," *IEEE Transactions on Vehicular Technology*, vol. 64, no. 12, pp. 5850–5865, Dec 2015.

[43] F. Liu *et al.*, "Dual-band femtocell traffic balancing over licensed and unlicensed bands," in *2012 IEEE International Conference on Communications (ICC)*, June 2012, pp. 6809–6814.

[44] S. Y. Lien, J. Lee, and Y. C. Liang, "Random access or scheduling: Optimum LTE Licensed-Assisted Access to unlicensed spectrum," *IEEE Communications Letters*, vol. 20, no. 3, pp. 590–593, March 2016.

[45] H. He *et al.*, "Proportional fairness-based resource allocation for LTE-U coexisting with Wi-Fi," *IEEE Access*, vol. 5, pp. 4720–4731, 2017.

[46] Y. Gu *et al.*, "Exploiting student-project allocation matching for spectrum sharing in LTE-unlicensed," in *2015 IEEE Global Communications Conference (GLOBECOM)*, Dec 2015, pp. 1–6.

[47] M. R. Khawer, J. Tang, and F. Han, "usICIC - a proactive small cell interference mitigation strategy for improving spectral efficiency of LTE networks in the unlicensed spectrum," *IEEE Transactions on Wireless Communications*, vol. 15, no. 3, pp. 2303–2311, March 2016.

[48] Z. Luo, M. Ding, and H. Luo, "CC on/off scheduling using learning-based prediction for LTE in the unlicensed spectrum," *IEEE Communications Letters*, vol. 19, no. 12, pp. 2158–2161, Dec 2015.

[49] C. Cano *et al.*, "Using LTE in unlicensed bands: Potential benefits and coexistence issues," *IEEE Communications Magazine*, vol. 54, no. 12, pp. 116–123, December 2016.

[50] H. Cui *et al.*, "LTE in the unlicensed band: Overview, challenges, and opportunities," *IEEE Wireless Communications*, vol. 24, no. 4, pp. 99–105, 2017.

[51] A. M. Voicu, L. Simi, and M. Petrova, "Inter-technology coexistence in a spectrum commons: A case study of Wi-Fi and LTE in the 5-GHz unlicensed band," *IEEE Journal on Selected Areas in Communications*, vol. 34, no. 11, pp. 3062–3077, Nov 2016.

[52] J. A. Sue *et al.*, "A binary time series model of LTE scheduling for machine learning prediction," in *2016 IEEE 1st International Workshops on Foundations and Applications of Self* Systems (FAS*W)*, Sept 2016, pp. 269–270.

[53] H. Luo *et al.*, "Quality-driven cross-layer optimized video delivery over LTE," *IEEE Communications Magazine*, vol. 48, no. 2, pp. 102–109, February 2010.

[54] S. Colonnese *et al.*, "Timely delivery versus bandwidth allocation for DASH-based video streaming over LTE," *IEEE Communications Letters*, vol. 20, no. 3, pp. 586–589, March 2016.

[55] A. Razzaq and A. Mehaoua, "Video transport over VANETs: Multi-stream coding with multi-path and network coding," in *IEEE Local Computer Network Conference*, Oct 2010, pp. 32–39.

[56] A. Razzaq and A. Mehaoua, "Layered video transmission using wireless path diversity based on Grey relational analysis," in *2011 IEEE International Conference on Communications (ICC)*, June 2011, pp. 1–6.

[57] Y. Cui, Z. Chang, and J. Huang, "Novel SVC bit-stream distribution alogrithm over wireless network," in *2011 4th IEEE International Conference on Broadband Network and Multimedia Technology*, Oct 2011, pp. 235–239.

[58] M. Condoluci *et al.*, "Multicast resource allocation enhanced by channel state feedbacks for multiple scalable video coding streams in LTE networks," *IEEE Transactions on Vehicular Technology*, vol. 65, no. 5, pp. 2907–2921, May 2016.

[59] S. Kumar *et al.*, "A three level adaptive video streaming framework over LTE," in *2016 IEEE International Conference on Systems, Man, and Cybernetics (SMC)*, Oct 2016, pp. 002 442–002 447.

[60] N. Khan and M. G. Martini, "QoE-based video delivery over LTE hierarchical architecture," in *2016 IEEE 27th Annual International Symposium on Personal, Indoor, and Mobile Radio Communications (PIMRC)*, Sept 2016, pp. 1–6.

[61] R. Zhang, S. L. Regunathan, and K. Rose, "Video coding with optimal inter/intra-mode switching for packet loss resilience," *IEEE Journal on Selected Areas in Communications*, vol. 18, no. 6, pp. 966–976, June 2000.

[62] K. C. J. Lin, S. P. Chou, and C. F. Chou, "Video multicast with heterogeneous user interests in multi-rate wireless networks," in *2012 IEEE Wireless Communications and Networking Conference (WCNC)*, April 2012, pp. 2092–2097.

[63] K. Stuhlmuller *et al.*, "Analysis of video transmission over lossy channels," *IEEE Journal on Selected Areas in Communications*, vol. 18, no. 6, pp. 1012–1032, June 2000.

[64] L. Badia *et al.*, "A Markov framework for error control techniques based on selective retransmission in video transmission over wireless channels," *IEEE Journal on Selected Areas in Communications*, vol. 28, no. 3, pp. 488–500, April 2010.

[65] S. Singh *et al.*, "Proximity-based video delivery architecture for LTE networks," *Electronics Letters*, vol. 52, no. 11, pp. 984–986, 2016.

[66] Q. Gong *et al.*, “Design and evaluation of a WiFi-direct based LTE cooperative video streaming system,” in *2016 IEEE Global Communications Conference (GLOBECOM)*, Dec 2016, pp. 1–6.

[67] W. Afifi, M. Hassan, and M. Krunz, “Enabling media streaming over LTE-U small cells,” in *2016 IEEE Wireless Communications and Networking Conference*, April 2016, pp. 1–6.

[68] 3GPP, “Study on Licensed-Assisted Access to unlicensed spectrum,” 3GPP, Tech. Rep. TR36.889, 2015.

[69] 3GPP, “Further advancements for E-UTRA (physical layer aspects),” 3GPP., Tech. Rep. TR 36.814 v9.0.0, 2010.

[70] ETSI, “Human factors (HF); quality of experience (QoE) requirements for real-time communication services,” European Telecommunications Standards Institute, Tech. Rep. TR 102 643 V1.0.1, 2009.

[71] M. Simon and M.-S. Alouinii, *Digital Communication Over Fading Channels : A Unified Approach to Performance Analysis*. New York: Wiley, 2000, pp. 219–234.

[72] Y. Collette and P. Siarry, *Multiobjective Optimization: Principles and Case Studies*. Berlin, Heidelberg: Springer Berlin Heidelberg, 2004, pp. 45–75.

Vita

Fatema Mahmood Aseeri was born in 1991, in Muharraq, Bahrain. She was educated in local public schools and graduated from Muharraq High School with honors in 2009. She attended the American University of Sharjah in the United Arab Emirates, from which she graduated magna cum laude, in 2015. Her degree was a Bachelor of Science in Electrical Engineering.

Ms. Aseeri began a Masters program in Electrical Engineering at the American University of Sharjah in 2015. She also worked as a Graduate Teaching Assistant at the American University of Sharjah and was a member of the university's Graduate Student Association.